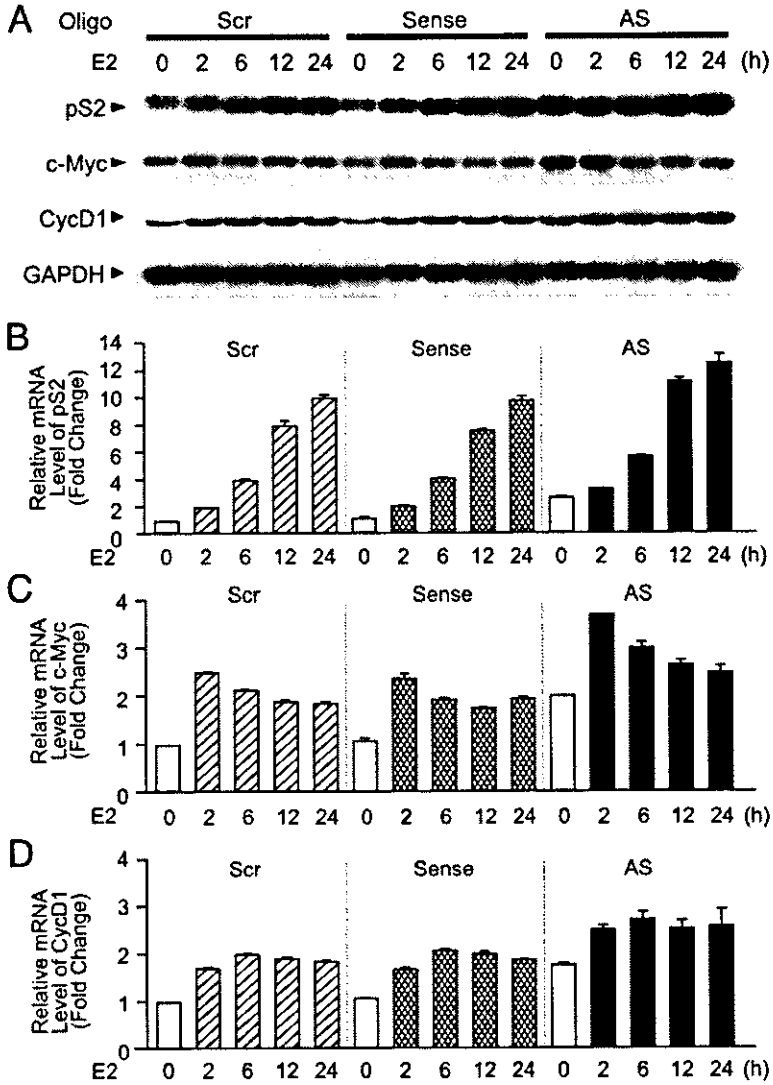


**Fig. 8.** PP5 AS Oligonucleotide Enhances $E_2$-Induced Transcription of Estrogen-Responsive Genes in MCF7 Cells

MCF7 cells were plated at a density of $1 \times 10^6$ cells per well on 10-cm plates and transfected with 5 $\mu$g control mismatch Scr, PP5 sense (Sense), or PP5 AS oligonucleotides for 12 h. Cells were serum starved for 24 h after the transfection and treated with $E_2$ (10 nM) for indicated times. Northern blot analysis was performed as indicated in Fig. 7. A, The representative result of three independent experiments of Northern blotting. B, C, and D, Quantification of mRNA levels of estrogen-responsive genes including pS2 (B), c-*myc* (C), and CycD1 (D) after normalization to GAPDH mRNA levels in MCF7 cells after $E_2$ treatment. Data are expressed as the mean ± SD values of fold change over control from three independent experiments. Data for cells transfected with Scr oligonucleotide and harvested at the starting point of $E_2$ treatments are used as control mRNA levels.

binding to ER$\alpha$ and ER$\beta$. The TPR domains of PP5 may also function as an autoinhibitory region against phosphatase activity as removal of the domain produces a marked increase in activity (31). In contrast, PP2A acts in a form of heterotrimer like other members of the PPP family, except PP5, and it has been reported that the catalytic subunit of the phosphatase is required for the interaction with ER$\alpha$. In regard to interacting functional domains of ERs, we have found E domains not containing an AD core region within AF-2 bind to PP5, whereas the A/B domain within AF-1 of ER$\alpha$ was reported to associate with PP2A. Thus it seems that ERs can be dephosphorylated by several kinds of protein phosphatases at different functional domains, leading to the more complex and subtle regulatory mechanisms for the receptors. Yet it is also noted that PP5 can exist in a native complex *in vivo* with the A subunit of PP2A via its TPR domains (20). It may be possible that PP5 directly interacts and cooperates with PP2A when the phosphatases bind to ERs and regulate the phosphorylation status of the receptors.

Notably, we showed that the truncated PP5 mutant consisting of only its TPR domains acts as a dominant negative PP5 because it increased the levels of ER$\alpha$ phosphorylation on S118 and transcriptional activation by ER$\alpha$ and ER$\beta$. Our data suggest a physiological

role for PP5 in ER signaling *in vivo*. It has been shown that the TPR domains of PP5 also have dominant negative effects on glucocorticoid receptor (GR)-mediated transactivation (16). PP5 could regulate the phosphorylation state of steroid receptors or associated phosphoproteins. We speculate that the TPR domains of PP5 may form complexes with endogenous PP5, leading to inhibition of phosphatase activity of endogenous PP5. Another possibility is that the TPR domains of PP5 displace other interacting proteins of steroid receptors, which are crucial for the regulation of the receptors. Indeed, some of the TPR-containing proteins appear to compete with each other for binding to heat shock protein 90, a major molecular chaperone that forms heterocomplexes with steroid receptors and participates in the signaling pathways of the receptors including glucocorticoid receptor (GR) and ER (32, 33).

To confirm endogenous PP5 activity toward ERα function, we used an AS strategy to decrease PP5 expression in MCF7 cells. The phosphorothioate AS oligonucleotide was designed to target the region overlapping the translation start site. Treatment with PP5 AS oligonucleotide, but not with control Scr or PP5 sense oligonucleotides, led to a significant reduction of PP5 expression (Fig. 6C) and a proportional increase in S118 phosphorylation of ERα (Fig. 5, C and D), transcriptional activity by ERα (Fig. 6C), and expression of estrogen-targeted gene mRNAs (Fig. 8, A–D) in MCF cells. In a report using PP5 AS oligonucleotide targeting the 3′-untranslated region of PP5 for MCF7 cells, Urban *et al.* (34) concluded that treatment with up to 500 nM of PP5 AS had no apparent effect on estrogen-induced expression of c-*myc* and cyclin D1 mRNA. In contrast to their Northern blot result, we investigated the time-dependent mRNA expression of estrogen-targeted genes and confirmed that PP5 AS oligonucleotide at a concentration less than 70 nM significantly suppressed $E_2$-dependent mRNA expression of pS2, c-*myc*, and cyclin D1. Thus, we consider that PP5 is a critical regulator of ER function that could modulate phosphorylation states and transcriptional activities of the receptors.

On the basis of its interactions with other proteins and of studies in which PP5 activity was inhibited using recombinant DNA approaches and antisense oligonucleotide treatment, potential biological roles of PP5 have begun to be elucidated. PP5 has been shown to modulate GR signaling (16, 35), to promote cell growth (34, 36), and to terminate responses to oxidative stress (17). In regard to oxidative stress, PP5 is a physiological inhibitor of apoptosis signal-regulating kinase 1-c-Jun N-terminal kinase/p38 pathway, which plays a pivotal role in stress-induced apoptosis (17). PP5 also interacts with the anaphase-promoting complex and preserves the dephosphorylated or inactivated state of the complex before the activation occurs (19). The growth-promoting effect of PP5 on cell proliferation appears to be exerted by inhibiting both glucocorticoid- and p53-mediated signaling pathways leading to $p21^{WAF1/Cip1}$-mediated growth arrest (35, 36). Constitutive overexpression of PP5 in MCF7 cells converted the $E_2$-dependent phenotype of the cells into an $E_2$-independent one (34). Indeed, we also observed that adenoviral delivery of PP5 into MCF7 cells increases the number of proliferating cells by cell cycle analysis, as it decreases the percentage of cells at $G_1$ phase and accumulates the cells at S phase (data not shown). Although it seems paradoxical, we speculate that the proliferative function of overexpressed PP5 observed in MCF7 cells may result from a hyperactivity of the enzyme to inhibit growth-arresting factors including GR and p53, which overcomes PP5-mediated inhibition of ER function at physiological concentrations of the phosphatase.

In summary, we have demonstrated that PP5 directly binds to ERs and regulates ER phosphorylation and transcriptional activity in a negative manner. The inhibitory action of PP5 against ER phosphorylation and function may contribute to a regulatory system of ER-mediated signaling at physiological and pathophysiological status. Further study will be required to understand the distinct activity of PP5 in estrogen-dependent cell proliferation, which may be responsible for developing hormone-dependent tumors.

## MATERIALS AND METHODS

### Yeast Two-Hybrid Screening

To analyze the regulatory mechanism of ERs, we employed the yeast two-hybrid system to search for proteins that bind to ERs by using ERβ (1–481), a truncated human ERβ cDNA fragment containing 1–481 amino acids (24) as a bait. The bait plasmid was constructed in-frame with the LexA DNA-binding domain of the pEG202NLS plasmid (Origene Technologies Inc., Rockville, MD). A cDNA library derived from estrogen-depleted MCF7 cells in the pJG4–5 prey plasmid was screened for proteins that interact with ERβ (1–481) using the EGY48 yeast reporter strain and the pSH18–34 LacZ reporter plasmid. Plasmids of positive clones were recovered, and the cDNA inserts were sequenced. To examine the interaction between ERβ (1–481) and PP5, ERβ (1–481) and PP5 constructs were cotransformed along with the pSH18–34 reporter plasmid into the EGY48 yeast strain. Transcriptional activation of LacZ gene was examined in X-gal (5-bromo-4-chloro-3-indolyl-β-D-galactopyranoside)-containing medium. As PP5 cDNA was included in a galactose-inducible vector, pJG4–5, the interaction between ERβ (1–481) and PP5 was observed when the reporter yeast was transformed with a ERβ (1–481) construct pEG202NLS-ERβ (1–481) and cultured in galactose-containing medium.

### GST Pull-Down Assay

GST constructs for full-length PP5 (GST-PP5) and truncated PP5 mutants GST-PP5 (2–71), GST-PP5 (28–165), GST-PP5 (2–181), GST-PP5 (2–132), and GST-PP5 (181–499), were prepared in pGEX4T-1 (Amersham Biosciences, Inc., Piscataway, NJ). With regard to structure of the truncated PP5 mutants, GST-PP5 (2–71) includes only one TPR domain. GST-PP5 (28–165) and GST-PP5 (2–181) contain four TPR

domains. GST-PP5 (2–312) consists of four TPR domains plus the N-terminal region of catalytic domain. GST-PP5 (181–499) includes the whole catalytic domain but not TPR domains. GST fusion proteins were induced, solubilized in solution A (20 mM Tris-HCl, pH 7.9; 10% glycerol; 80 mM KCl; 1 mM $MgCl_2$; 0.2 mM EDTA; 0.5 mM dithiothreitol; 0.5 mM phenylmethylsulfonyl fluoride; and 1% Triton X-100), and bound to glutathione-Sepharose 4B beads following the manufacturer's instruction (Amersham Biosciences, Inc.). GST fusion proteins bound to glutathione beads were incubated at 4 C for 1.5 h with $^{35}$S-labeled ERα or ERβ, which was synthesized *in vitro* using the TnT-coupled reticulocyte lysate system (Promega Corp., Madison, WI). After the incubation, the beads were washed three times with solution A, and the complexes were separated by SDS-PAGE. The results were visualized using a Fuji FLA 3000 phosphoimaging analyzer (Fuji Film, Tokyo, Japan).

### Mammalian Two-Hybrid Assay

The luciferase reporter plasmid TK-MH100 × 4Luc and the expression plasmids pCMX-GAL4 and pCMX-VP16 were kindly provided by K. Umesono (Kyoto University, Kyoto, Japan). pCMX-VP16-PP5 was constructed by an in-frame ligation of human PP5 cDNA to the VP16 transactivation domain in pCMX-VP16. pCMX-GAL4 constructs were generated by in-frame ligations of various ERα and ERβ cDNA fragments to the GAL4 DNA binding domain in pCMX-GAL4. The receptor domains encoded by ERα and ERβ cDNA fragments were as follows: for ERα, ABCD (amino acids 1–302), ABC (amino acids 1–263), E (amino acids 302–530), and a part of EF (amino acids 530–595) domains; for ERβ, ABCD (amino acids 1–248), ABC (amino acids 1–213), E (amino acids 248–481), and a part of EF (amino acids 481–530) domains. 293T cells were plated at a density of $6 \times 10^4$ cells per well of 24-well plates and incubated overnight. Cells were then cotransfected with plasmids containing 0.8 μg TK-MH100 × 4Luc, 0.7 μg pRL-TK vector (Promega), 0.2 μg VP16-PP5, and 0.1 μg GAL4 fusion constructs of ERα or ERβ using FuGENE 6 transfection reagent (Roche Diagnostics, Indianapolis, IN). Cells were cultured for 24 h and luciferase assays were performed using a Dual-Luciferase Assay System (Promega). Data are expressed as the mean ± SD of three independent experiments performed in triplicate.

### Coimmunoprecipitation Assay

The GFP-tagged ERα construct was generated by an in-frame ligation of human ERα cDNA to downstream of GFP in pEGFP-C2 (BD Biosciences CLONTECH, Palo Alto, CA). The Flag-tagged pcDNA3 (Invitrogen, San Diego, CA) constructs pcDNA3-Flag-PP5 and pcDNA3-Flag-TPR were prepared by insertions of full-length PP5 and TPR domains (amino acids 28–165) into pcDNA3 containing Flag tag. 293T cells were plated at a density of $1 \times 10^6$ cells per dish in 10-cm dishes and cotransfected with 7.5 μg GFP-ERα and 7.5 μg Flag-PP5 or Flag-TPR by the calcium phosphate method. After 24 h, cells were incubated with PBS containing 5 mM hybrophobic lysine-specific cross-linker dithiobis[succinimidyl propionate] (Pierce Biotechnology, Inc., Rockford, IL) at 4 C for 30 min. The reaction was stopped by addition of 100 mM Tris-HCl, pH 7.5, at room temperature for 10 min. Cells were washed with PBS and lysed in immunoprecipitation buffer (50 mM Tris-HCl, pH 7.5, 150 mM NaCl, 1% Nonidet P-40, 0.5 mM aprotinin, 0.5 mM phenylmethylsulfonylfluoride). Lysates were cleared by centrifugation, and protein concentrations were determined by the Bradford method (Bio-Rad Laboratories, Inc., Hercules, CA). For immunoprecipitation, 1 mg of lysates were incubated with 10 μg of anti-Flag antibody M2 (Sigma Chemical Co., St. Louis, MO) for 3 h at 4 C, and then incubated with 20 μl of protein G-Sepharose beads (50% vol/vol slurry) (Amersham Biosciences, Inc.) for 90 min at 4 C. The beads were washed three times with immunoprecipitation buffer and resuspended in 20 μl of sample buffer for SDS-PAGE. Eluted proteins were subjected to SDS-PAGE, followed by electroblotting onto polyvinylidene difluoride membrane, and probed with antibodies against GFP (Medical & Biological Laboratories Co., Ltd., Nagoya, Japan). The antibody-antigen complexes were detected using the enhanced chemiluminescence system (Amersham Biosciences, Inc.) according to the manufacturer's instruction. In experiments for examining the interaction between endogenous PP5 and ERα, the extracts from MCF7 cells were immunoprecipitated with an anti-PP5 antibody PP5/PPT (BD Biosciences, San Jose, CA) or nonimmune serum and probed by an anti-ERα antibody H-184 (Santa Cruz Biotechnology, Santa Cruz, CA).

### Adenoviral Gene Expression

Adenoviral constructs of Flag-tagged human PP5 (Ad-PP5) and GFP-fusion histone H2B (Ad-GFP) were prepared in an adenovirus vector using Adenovirus Expression Vector Kit (Takara Bio Inc., Shiga, Japan) (37, 38). MCF7 cells were infected with the recombinant adenoviruses at a multiplicity of infection (MOI) of 10 for 12 h. The infected cells were serum starved for 24 h in phenol red-free DMEM and treated with 10 nM $E_2$ in DMEM containing 10% dextran-coated charcoal-treated fetal calf serum (dccFCS) for the indicated times.

### Oligonucleotide Treatment

Twenty-three-base phosphorothioate oligonucleotides were prepared by Invitrogen. Sequences for PP5 AS, PP5 sense, and control Scr oligonucleotides were 5′-CTCTCGCCCTC-CGCCATCGCCAT-3′, 5′-ATGGCGATGGCGGAGGGCGAGAG-3′, and 5′-GCAGTGGCGAGCTGAGAGAGGGG-3′, respectively. MCF7 cells were incubated with phenol red-free DMEM containing 10% dccFCS before experiments. Cells were transfected with oligonucleotides using GeneSilencer reagent (GeneTherapy Systems, Inc., San Diego, CA) according to the procedure recommended by the manufacturer. Twelve hours after transfection, cells were fed with serum-starved DMEM, or phenol red-free DMEM containing 10% dccFCS supplemented with or without $E_2$. Cells were used for experiments involving ER phosphorylation, transactivation, and expression of estrogen target genes.

### Transcription Assay of ER

Expression vectors of S118A (HE457) and S118E (HE458) mutants of ERα were the gifts from Dr. P. Chambon (3). N-terminal Flag-tagged pcDNA3 constructs including full-length PP5, TPR domains, and catalytic domain were generated. 293T cells at a density of $1 \times 10^4$ cells per well on 24-well plates were transfected with 0.8 μg ERE-tk-Luc, 0.7 μg pRL-CMV (Promega), 5 ng of expression vectors for full-length ERα/ERβ or ERα mutants, and 0–50 ng of expression vectors for full-length or truncated PP5 in phenol red-free DMEM containing 10% dccFCS using FuGENE 6 transfection reagent (Roche Diagnostics). Twelve hours after transfection, cells were treated with or without 10 nM $E_2$ for 24 h and luciferase assays were performed. Data were represented as the mean ± SD of three independent experiments performed in triplicate.

### Northern Blot Analysis and Probes

The cDNAs encoding full-length human pS2, human c-*myc*, human cyclin D1, and human GAPDH were cloned by RT-PCR and verified by sequencing. Probes for Northern blot analysis were prepared by labeling the cloned cDNAs with [α-$^{32}$P]dCTP using the Random Primer Labeling Kit (Takara

Bio Inc.). Total RNAs (20 μg) were separated in 1% formaldehyde denaturing agarose gels and transferred to Hybond-NX membranes (Amersham Biosciences, Inc.). Blotted membranes were hybridized with the $^{32}$P-labeled probes in a hybridization buffer (0.1% sodium dodecyl sulfate (SDS), 50% formamide, 5× sodium saline citrate (SSC), 50 mM $NaPO_4$ (pH 6.8), 0.1% sodium pyrophosphate, 5 × Denhardt's solution, and 50 μg/ml salmon sperm DNA] at 42 C overnight. Membranes were then washed with 2× SSC, 0.1% SDS at 42 C for 30 min and 0.2× SSC, 0.1% SDS at 42 C for 30 min. Radioactivities of the signals were quantified using a Fuji FLA 3000 phosphoimaging analyzer (Fuji Photo Film, Tokyo, Japan). The mRNA levels for estrogen-targeted genes at each time point were determined by the signal intensities normalized by that of GAPDH mRNA level in an identical sample. Data for cells treated with vehicle and harvested at the starting point of $E_2$ treatments are used as control mRNA levels. Data are expressed as the mean ± SD values of fold change over control from three independent experiments.

### Analysis for Phosphorylation State of ERα at S118

MCF7 cells were plated at a density of 1.4 × $10^5$ cells on six-well plates and transfected with 1 μg of expression plasmids for full-length PP5, TPR domains, or an empty vector for 12 h using FuGENE 6 transfection reagent (Roche Diagnostics). In experiments using oligonucleotides, cells were transfected with PP5 sense, AS, or control mismatch Scr oligonucleotides for 12 h using GeneSilencer reagent. In a preliminary experiment, we confirmed that the transfection efficiency of pEGFP-C1 vector (BD Biosciences CLONTECH) into MCF7 cells was 32% using FuGENE 6 transfection reagent. Transfected cells were serum starved for 24 h and treated with $E_2$ (10 nM), EGF(100 ng/ml), or vehicles. Cell extracts were subjected to immunoblotting using a specific antibody against phosphorylated ERα at S118 (16J4)(Cell Signaling Technology, Beverly, MA). Quantification of signal intensities was performed using LAS 1000 image analyzer (Fuji Photo Film). Three independent experiments were performed, and phosphorylation levels at ERα S118 were normalized by total protein amounts of ERα.

### Cell Cycle Analysis

For flow cytometry analysis, MCF7 cells were transduced with recombinant adenoviruses Ad-PP5 or Ad-GFP. Twelve hours after infection, cells were cultured in serum-deleted medium for 24 h and treated with $E_2$ (10 nM). Cells were trypsinized, fixed with 70% ethanol, treated with RNase A (100 μg/ml), and then stained with propidium iodide (10 μg/ml). Cells were analyzed by FACS Calibur flow cytometer (Becton Dickinson and Co., Mountain View, CA) and the cell-cycle profile was determined using ModFit LT software (Becton Dickinson).

## Acknowledgments

We thank Dr. P. Chambon for kindly providing HE457 and HE458 plasmids, and T. Hishinuma, T. Ichikawa, and A. Harashima for their technical assistance.

Received August 9, 2003. Accepted January 27, 2004.

Address all correspondence and requests for reprints to: Satoshi Inoue, Division of Gene Regulation and Signal Transduction, Research Center for Genomic Medicine, Saitama Medical School, 1397-1 Yamane, Hidaka-shi, Saitama 350-1241, Japan. E-mail: INOUE-GER@h.u-tokyo.ac.jp.

This work was supported in part by grants-in-aid from the Ministry of Health, Labor and Welfare; from the Ministry of Education, Culture, Sports, Science and Technology of Japan; from Kanzawa Medical Research Foundation; and from Novartis Foundation (Japan) for the Promotion of Science.

## REFERENCES

1. Muramatsu M, Inoue S 2000 Estrogen receptors: how do they control reproductive and nonreproductive functions? Biochem Biophys Res Commun 270:1–10
2. Shao D, Lazar MA 1999 Modulating nuclear receptor function: may the phos be with you. J Clin Invest 103: 1617–1618
3. Ali S, Metzger D, Bornert JM, Chambon P 1993 Modulation of transcriptional activation by ligand-dependent phosphorylation of the human oestrogen receptor A/B region. EMBO J 12:1153–1160
4. Kato S, Endoh H, Masuhiro Y, Kitamoto T, Uchiyama S, Sasaki H, Masushige S, Gotoh Y, Nishida E, Kawashima H, Metzger D, Chambon P 1995 Activation of the estrogen receptor through phosphorylation by mitogen-activated protein kinase. Science 270:1491–1494
5. Tremblay A, Tremblay GB, Labrie F, Giguere V 1999 Ligand-independent recruitment of SRC-1 to estrogen receptor β through phosphorylation of activation function AF-1. Mol Cell 3:513–519
6. Chen D, Pace PE, Coombes RC, Ali S 1999 Phosphorylation of human estrogen receptor α by protein kinase A regulates dimerization. Mol Cell Biol 19:1002–1015
7. Chen D, Riedl T, Washbrook E, Pace PE, Coombes RC, Egly JM, Ali S 2000 Activation of estrogen receptor α by S118 phosphorylation involves a ligand-dependent interaction with TFIIH and participation of CDK7. Mol Cell 6:127–137
8. Le Goff P, Montano MM, Schodin DJ, Katzenellenbogen BS 1994 Phosphorylation of the human estrogen receptor. Identification of hormone-regulated sites and examination of their influence on transcriptional activity. J Biol Chem 269:4458–4466
9. Joel PB, Traish AM, Lannigan DA 1998 Estradiol-induced phosphorylation of serine 118 in the estrogen receptor is independent of p42/p44 mitogen-activated protein kinase. J Biol Chem 273:13317–13323
10. Barford D, Das AK, Egloff MP 1998 The structure and mechanism of protein phosphatases: insights into catalysis and regulation. Annu Rev Biophys Biomol Struct 27:133–164
11. Cohen PT 1997 Novel protein serine/threonine phosphatases: variety is the spice of life. Trends Biochem Sci 22:245–251
12. Chen MX, McPartlin AE, Brown L, Chen YH, Barker HM, Cohen PT 1994 A novel human protein serine/threonine phosphatase, which possesses four tetratricopeptide repeat motifs and localizes to the nucleus. EMBO J 13: 4278–4290
13. Hirano T, Kinoshita N, Morikawa K, Yanagida M 1990 Snap helix with knob and hole: essential repeats in *S. pombe* nuclear protein nuc2+. Cell 60:319–328
14. Sikorski RS, Boguski MS, Goebl M, Hieter P 1990 A repeating amino acid motif in CDC23 defines a family of proteins and a new relationship among genes required for mitosis and RNA synthesis. Cell 60:307–317
15. Blatch GL, Lassle M 1999 The tetratricopeptide repeat: a structural motif mediating protein-protein interactions. Bioessays 21:932–939
16. Chen MS, Silverstein AM, Pratt WB, Chinkers M 1996 The tetratricopeptide repeat domain of protein phosphatase 5 mediates binding to glucocorticoid receptor heterocomplexes and acts as a dominant negative mutant. J Biol Chem 271:32315–32320
17. Morita K, Saitoh M, Tobiume K, Matsuura H, Enomoto S, Nishitoh H, Ichijo H 2001 Negative feedback regulation of

ASK1 by protein phosphatase 5 (PP5) in response to oxidative stress. EMBO J 20:6028–6036
18. Chinkers M 1994 Targeting of a distinctive protein-serine phosphatase to the protein kinase-like domain of the atrial natriuretic peptide receptor. Proc Natl Acad Sci USA 91:11075–11079
19. Ollendorff V, Donoghue DJ 1997 The serine/threonine phosphatase PP5 interacts with CDC16 and CDC27, two tetratricopeptide repeat-containing subunits of the anaphase-promoting complex. J Biol Chem 272:32011–32018
20. Lubert EJ, Hong Y, Sarge KD 2001 Interaction between protein phosphatase 5 and the A subunit of protein phosphatase 2A: evidence for a heterotrimeric form of protein phosphatase 5. J Biol Chem 276:38582–38587
21. Brzozowski AM, Pike AC, Dauter Z, Hubbard RE, Bonn T, Engstrom O, Ohman L, Greene GL, Gustafsson JA, Carlquist M 1997 Molecular basis of agonism and antagonism in the oestrogen receptor. Nature 389:753–758
22. Shiau AK, Barstad D, Loria PM, Cheng L, Kushner PJ, Agard DA, Greene GL 1998 The structural basis of estrogen receptor/coactivator recognition and the antagonism of this interaction by tamoxifen. Cell 95:927–937
23. Pike AC, Brzozowski AM, Hubbard RE, Bonn T, Thorsell AG, Engstrom O, Ljunggren J, Gustafsson JA, Carlquist M 1999 Structure of the ligand-binding domain of oestrogen receptor $\beta$ in the presence of a partial agonist and a full antagonist. EMBO J 18:4608–4618
24. Ogawa S, Inoue S, Orimo A, Hosoi T, Ouchi Y, Muramatsu M 1998 Cross-inhibition of both estrogen receptor $\alpha$ and $\beta$ pathways by each dominant negative mutant. FEBS Lett 423:129–132
25. Brown AM, Jeltsch JM, Roberts M, Chambon P 1984 Activation of pS2 gene transcription is a primary response to estrogen in the human breast cancer cell line MCF-7. Proc Natl Acad Sci USA 81:6344–6348
26. Dubik D, Shiu RP 1992 Mechanism of estrogen activation of c-myc oncogene expression. Oncogene 7:1587–1594
27. Sabbah M, Courilleau D, Mester J, Redeuilh G 1999 Estrogen induction of the cyclin D1 promoter: involvement of a cAMP response-like element. Proc Natl Acad Sci USA 96:11217–11222
28. Castro-Rivera E, Samudio I, Safe S 2001 Estrogen regulation of cyclin D1 gene expression in ZR-75 breast cancer cells involves multiple enhancer elements. J Biol Chem 276:30853–30861
29. Smith CL 1998 Cross-talk between peptide growth factor and estrogen receptor signaling pathways. Biol Reprod 58:627–632
30. Lu Q, Surks HK, Ebling H, Baur WE, Brown D, Pallas DC, Karas RH 2003 Regulation of estrogen receptor $\alpha$-mediated transcription by a direct interaction with protein phosphatase 2A. J Biol Chem 278:4639–4645
31. Sinclair C, Borchers C, Parker C, Tomer K, Charbonneau H, Rossie S 1999 The tetratricopeptide repeat domain and a C-terminal region control the activity of Ser/Thr protein phosphatase 5. J Biol Chem 274:23666–23672
32. Owens-Grillo JK, Hoffmann K, Hutchison KA, Yem AW, Deibel Jr MR, Handschumacher RE, Pratt WB 1995 The cyclosporin A-binding immunophilin CyP-40 and the FK506-binding immunophilin hsp56 bind to a common site on hsp90 and exist in independent cytosolic heterocomplexes with the untransformed glucocorticoid receptor. J Biol Chem 270:20479–20484
33. Ratajczak T, Carrello A 1996 Cyclophilin 40 (CyP-40), mapping of its hsp90 binding domain and evidence that FKBP52 competes with CyP-40 for hsp90 binding. J Biol Chem 271:2961–2965
34. Urban G, Golden T, Aragon IV, Scammell JG, Dean NM, Honkanen RE 2001 Identification of an estrogen-inducible phosphatase (PP5) that converts MCF-7 human breast carcinoma cells into an estrogen-independent phenotype when expressed constitutively. J Biol Chem 276:27638–27646
35. Zuo Z, Urban G, Scammell JG, Dean NM, McLean TK, Aragon I, Honkanen RE 1999 Ser/Thr protein phosphatase type 5 (PP5) is a negative regulator of glucocorticoid receptor-mediated growth arrest. Biochemistry 38: 8849–8857
36. Zuo Z, Dean NM, Honkanen RE 1998 Serine/threonine protein phosphatase type 5 acts upstream of p53 to regulate the induction of p21(WAF1/Cip1) and mediate growth arrest. J Biol Chem 273:12250–12258
37. Niwa H, Yamamura K, Miyazaki J 1991 Efficient selection for high-expression transfectants with a novel eukaryotic vector. Gene 108:193–199
38. Miyake S, Makimura M, Kanegae Y, Harada S, Sato Y, Takamori K, Tokuda C, Saito I 1996 Efficient generation of recombinant adenoviruses using adenovirus DNA-terminal protein complex and a cosmid bearing the full-length virus genome. Proc Natl Acad Sci USA 93:1320–1324

***Molecular Endocrinology*** **is published monthly by The Endocrine Society (http://www.endo-society.org), the foremost professional society serving the endocrine community.**

JOURNAL OF BONE AND MINERAL RESEARCH
Volume 19, Number 8, 2004
Published online on March 29, 2004; doi: 10.1359/JBMR.040324


# Association of Multiple Nucleotide Variations in the Pituitary Glutaminyl Cyclase Gene (*QPCT*) With Low Radial BMD in Adult Women

Yoichi Ezura,[1] Mitsuko Kajita,[1] Ryota Ishida,[1] Shoko Yoshida,[1,2] Hideyo Yoshida,[3,4] Takao Suzuki,[3,4] Takayuki Hosoi,[3,4] Satoshi Inoue,[5] Masataka Shiraki,[6] Hajime Orimo,[3,4] and Mitsuru Emi[1]

**ABSTRACT: Correlation between 13 genetic variations of the *glutaminyl-peptide cyclotransferase* gene and adjusted aBMD was tested among 384 adult women. Among 13 variations with strong linkage disequilibrium, R54W showed a prominent association ($p = 0.0003$), which was more striking when examined among 309 elder subjects (≥50 years; $p = 0.0001$). Contribution for postmenopausal bone loss was suggested.**

**Introduction:** Alterations in homeostatic regulation of estrogen through the hypothalamus-pituitary-gonadal axis (HPG axis) importantly affect the pathogenesis of osteoporosis. Osteoporosis-susceptibility genes have been proposed in this hormonal axis, such as estrogen receptor genes and the gonadotropin-releasing hormone gene (*GnRH*). Here we report another example of genes: glutaminyl-peptide cyclotransferase gene (*QPCT*), an essential modifier of pituitary peptide hormones, including GnRH.
**Materials and Methods:** Analyses of association of 13 single nucleotide polymorphisms (SNPs) at the *QPCT* locus with adjusted areal BMD (adj-aBMD) were carried out among 384 adult women. Linkage disequilibrium (LD) was analyzed by haplotype estimation and calculation of $D'$ and $r^2$. Multiple regression analysis was applied for evaluating the combined effects of the variations.
**Results and Conclusions:** LD analysis indicated strong linkage disequilibrium within the entire 30-kb region of the *QPCT* gene. Significant correlations were observed between the genotypes of the six SNPs and the radial adj-aBMD, among which R54W (nt + 160C>T) presented the most prominent association ($p = 0.0003$). Striking association was observed for these SNPs among the 309 subjects >50 years of age (R54W, $p = 0.0001$; −1095T>C, $p = 0.0002$; −1844C>T, $p = 0.0002$). Multiple regression analyses indicated that multiple SNPs in the gene might act in combination to determine the radial adj-aBMD. These results indicate that genetic variations in *QPCT* are the important factors affecting the BMD of adult women that contribute to susceptibility for osteoporosis. The data should provide new insight into the etiology of the disease and may suggest a new target to be considered during treatment.
**J Bone Miner Res 2004;19:1296–1301. Published online on March 29, 2004; doi: 10.1359/JBMR.040324**

**Key words: single nucleotide polymorphism, glutaminyl-peptide cyclotransferase gene, pituitary glutaminyl cyclase, BMD, association study, quantitative trait**

## INTRODUCTION

OSTEOPOROSIS IS A MULTIFACTORIAL common disease characterized by reduced bone mass, microarchitectual deterioration of bone tissue, and increased risk of fragility fractures. Nucleotide variations in several genes that play roles in the pathogenesis of osteoporosis, acting in combination, may explain the complexity of variations in BMD in a population.[1,2] However, the details of these covariates have not been clarified.

Adequate levels of sex hormones, especially estrogen, are essential for achievement of peak bone mass as well as for postmenopausal maintenance of the skeletal system.[3] A hierarchical regulatory system, the hypothalamic-pituitary-gonadal axis (HPG axis), controls serum levels of these hormones.[4–6] Recently, we showed that an amino acid variation (W16S) in the signal peptide of gonadotropin-releasing hormone (*GnRH*), a primary regulator of the HPG axis, was associated with BMD in postmenopausal women.[7] Those results suggested that variations in other genes involved in the HPG axis could also affect BMD and influence susceptibility to osteoporosis.

The authors have no conflict of interest.

[1]Department of Molecular Biology, Institute of Gerontology, Nippon Medical School, Kawasaki, Japan; [2]Department of Molecular Genetic Sciences, Division of Biomedical Laboratory Sciences, Graduate School of Allied Health Sciences, Tokyo Medical and Dental University, Tokyo, Japan; [3]Department of Epidemiology, Tokyo Metropolitan Institute of Gerontology and Geriatric Hospital, Tokyo, Japan; [4]Department of Internal Medicine, Tokyo Metropolitan Institute of Gerontology and Geriatric Hospital, Tokyo, Japan; [5]Department of Geriatric Medicine, Faculty of Medicine, University of Tokyo, Tokyo, Japan; [6]Department of Internal Medicine, Research Institute and Practice for Involutional Diseases, Nagano, Japan.

TABLE 1. PHYSICAL AND CLINICAL CHARACTERISTICS OF THE 384 SUBJECTS

| | *Whole* | *Younger subjects (age ≤ 50 years)* | *Elder subjects (age > 50 years)* |
|---|---|---|---|
| Number | 384 | 75 | 309 |
| Age (years) | 58.4 ± 8.58 (32–69) | 44.9 ± 4.59 (32–50) | 61.7 ± 5.61 (51–69) |
| Weight (kg) | 54.2 ± 8.91 (28.8–89.0) | 56.7 ± 8.63 (40.5–89.0) | 53.6 ± 8.88 (28.8–84.5) |
| BMI (kg/m$^2$) | 23.7 ± 3.61 (14.7–38.5) | 23.5 ± 3.79 (17.5–38.5) | 23.7 ± 3.57 (14.7–37.7) |
| Height (cm) | 151.3 ± 5.85 (130.5–169.0) | 155.3 ± 5.21 (146–169) | 150.4 ± 5.58 (130.5–163.4) |
| Raw aBMD (g/cm$^2$)* | 0.399 ± 0.082 (0.178–0.635) | 0.488 ± 0.060 (0.369–0.635) | 0.378 ± 0.072 (0.178–0.581) |
| Adjusted aBMD (g/cm$^2$)† | 0.399 ± 0.054 (0.225–0.554) | 0.403 ± 0.050 (0.280–0.504) | 0.398 ± 0.056 (0.225–0.554) |

*Radial BMD was measured by areal scan with DTX-200.
†Raw aBMD data was adjusted with age and BMI by multiple regression analysis.

Active forms of the small peptide hormones secreted by the hypothalamus and pituitary, such as GnRH and thyrotropin releasing hormone (TRH), are susceptible to proteolytic degradation. However, protection from proteolysis occurs in situ, when required, through modification of the N-terminal or C-terminal ends of the peptides.[8–10] GnRH and TRH are glutaminyl peptides in which the N-terminal glutamine residue is associated with histidine in the next position.[8,11] For protection, an enzyme designated pituitary glutaminyl cyclotransferase (QPCT, also known as pituitary glutaminyl cyclase; EC 2.3.2.5) converts the N-terminal glutamine of these peptides into the pyroglutamate (5-oxoproline or pyrrolidone carboxylic acid), forming a cyclic amide structure by dehydration.[8,9] The gene encoding this enzyme (*QPCT*) lies on chromosome 2p22.3, within the region where a quantitative trait locus (QTL) for forearm BMD has been identified in the Chinese population (2p21.1–24)[12] and near a QTL for spinal BMD identified among whites (2p23–24).[13] Thus, biological and genetic evidence leads us to hypothesize that differences in bone mass among individuals from the general population might be influenced by common nucleotide variation(s) of the *QPCT* gene.

In the work reported here, we examined the potential involvement of the *QPCT* gene in the pathogenesis of osteoporosis by investigating 13 known polymorphisms and by analyzing linkage disequilibrium (LD) among these variations after constructing haplotypes. Multiple regression analyses were carried out to examine possible associations of genotypes or haplotypes with BMD in 384 Japanese women.

## MATERIALS AND METHODS

### *Subjects*

DNA samples were obtained from peripheral blood of 384 unrelated women from the general Japanese population. Mean ages and body mass indices (BMIs) were 58.4 ± 8.6 years (SD; range, 32–69 years) and 23.7 ± 3.61 kg/m$^2$ (range, 14.7–38.5 kg/m$^2$). The areal BMD of distal radius (expressed in g/cm$^2$) in each participant was measured by DXA using a DTX-200 (Osteometer Meditech, Hawthorne, CA, USA). In this study, we use a specific abbreviation "aBMD" to denote the DXA measurement of the standard "areal BMD" for our results. Although volumetric analysis of BMD was not applied in this study, there were no large differences in bone size among our study subjects, and the measured aBMD was normalized for differences in age, height, and weight using the Instat 3 software package (GraphPad Software, San Diego, CA, USA) and multiple regression analysis.[7,14] The adjustment equation for the study subjects was as follows: adj-aBMD (g/cm$^2$) = measured-aBMD (g/cm$^2$) − 0.006375 × [58.39 − age (years)] + 0.008961 × [23.65 − BMI (kg/cm$^2$)]. The aBMD in the radius was measured according to the Guidelines for Osteoporosis Screening in a health check-up program in Japan.[15] No participant had medical complications or was undergoing treatment for conditions known to affect bone metabolism, such as pituitary disease, hyperthyroidism, primary hyperparathyroidism, renal failure, adrenal disease, or rheumatic disease, and none were receiving estrogen replacement therapy. The study received institutional review board approval from participating collection sites. All participants were nonrelated volunteers, and written informed consent was obtained from all human subjects.

The effect of sex hormones on changes in BMD may be important during skeletal development and/or during the postmenopausal period.[16,17] To analyze separately the period when genotypes might contribute most to lowering adj-aBMD, we divided the 384 subjects into younger and older groups: >50 years ($n$ = 309) and ≤50 years ($n$ = 75). Basic characteristics of the subjects are summarized in Table 1.

### *Single nucleotide polymorphism selection and genotyping*

Thirteen polymorphic variations of the *QPCT* gene (Table 2) were extracted from the dbSNP of the NCBI (http://www.ncbi.nlm.nih.gov/SNP/) and from the JSNP database (http://snp.ims.u-tokyo.ac.jp/index.html), spanning almost the entire 30-kb region of the gene locus. Genotypes for nine of these single nucleotide polymorphism [SNPs; IVS1 + 3583C>G, IVS1–3796A>G, IVS1–1629G>C, R54W (nt + 160C>T), IVS2–42A>G, IVS4 + 974G>A, IVS4 + 1053T>C, IVS4–1132C>A, and IVS6 + 73A>G] were determined by the single-base extension method,[18,19] according to the manufacturer's instructions for the SNaPshot kit (Applied Biosystems, Foster City, CA, USA). In brief, a ~600-bp region of genomic DNA covering the sequence surrounding each of the target SNPs was amplified by a standard PCR program. The PCR products were purified

TABLE 2. SUMMARY OF POLYMORPHISMS ANALYZED AT THE QPCT LOCUS

| *No.* | *Name* | *nt.* | *Location* | *dbSNP** |
|---|---|---|---|---|
| 1 | −2300C>T | C/T | Promoter | rs952712 |
| 2 | −1844C>T | C/T | Promoter | rs3755192 |
| 3 | −1095T>C | T/C | Promoter | rs3755191 |
| 4 | IVS1+3583C>G | C/G | Intron 1 | rs3770753 |
| 5 | IVS1−3796A>G | A/G | Intron 1 | rs3770752 |
| 6 | IVS1−1629G>C | G/C | Intron 1 | rs3770751 |
| 7 | +126C>T (Y42Y) | taC/taT | Exon 1 | rs2302652 |
| 8 | +160C>T (R54W) | Cgg/Tgg | Exon 2 | rs2255991 |
| 9 | IVS2−42A>G | A/G | Intron 2 | rs2302651 |
| 10 | IVS4+974G>A | G/A | Intron 4 | rs3770748 |
| 11 | IVS4+1053T>C | T/C | Intron 4 | rs3770747 |
| 12 | IVS4−1132C>A | C/A | Intron 4 | rs1468816 |
| 13 | IVS6+73A>G | A/G | Intron 6 | rs2287094 |

*Number from dbSNP database of NCBI (http://www.ncbi.nlm.nih.gov/SNP/).

using a separation system (Millipore Japan, Tokyo, Japan) before the single-base primer extension reactions were performed with fluorescence-labeled di-deoxynucleotides (ddNTPs). The extension products were dephosphorylated with shrimp alkaline phosphatase to eliminate co-migration with unincorporated substrates (Roche Japan, Tokyo, Japan). Signals were detected using an ABI377 system and GeneScan Analysis Software vr2.1 (Applied Biosystems). The Invader assay (Third Wave Technologies, Madison, WI, USA)[20,21] was used to genotype the other four SNPs (−2300C>T, −1844C>T, −1095T>C, and R54W) according to the manufacturer's protocol. In brief, regions flanking each SNP (e.g., for −2300C>T, a 599-bp region surrounding the SNP to include nucleotides 374132 to 374730 in NT_005367.1) were amplified from 10 ng of genomic DNA by a standard PCR protocol, using the following primer sets: −2300C>T, forward 5′-TGCAAGCGGCTTTCCAG-3′ and reverse 5′-CCTTCATTTCCTTCACATCACAG-3′; −1844C>T, forward 5′-ACAGCTCCTCTCTTGCTGCC-3′ and reverse 5′-CCGCTTGCAGGAAATCACTC-3′; −1095T>C, forward 5′-TTCCACAGTGAGGATCAGGG-3′ and reverse 5′-CAGCCACTCAGGAAATGCAC-3′; R54W, forward 5′-ACTTAATTGGGAGCCTCGGG-3′ and reverse 5′-CCTCATTTGACATAAAGTTCTCCC-3′.

After dilution (1:333) in distilled water, 1 μl of each product was used as template in a 6-μl reaction mixture for the Invader assay on 384-well plates, along with appropriate amounts of the probe mix, FRET mix, and Cleavase XI Enzyme in $MgCl_2$ buffer. The manufacturer provided the designed probe sets along with the required reagents. A 5-minute denaturation was followed by a 60-minute incubation at 63°C in an ABI9700 thermal cycler (Applied Biosystems). No mineral oil was used. The fluorescence signals (for FAM, excitation 485/20 nm and emission 530/25 nm; for Redmond Red, excitation 560/20 nm and emission 620/40 nm) were detected by a CytoFluor 4000 multiwell plate reader (Applied Biosystems). A Hydra microdispenser (Robbins Scientific Corp., Sunnyvale, CA, USA) was used for liquid handling.

*Haplotyping, linkage disequilibrium, and statistical analysis*

Haplotype frequencies among the 768 alleles investigated were calculated by Arlequine software (Genetics and Biometry Laboratory, Geneva, Switzerland). LD for all possible two-way combinations of the SNPs was tested with $D$, $D'$, and $r^2$.[22,23]

Quantitative associations between genotypes and adj-aBMD values (g/cm$^2$) were analyzed by ANOVA with regression analysis as a post hoc test. The three genotypic categories of each SNP (e.g., C/C, C/T, and T/T for rs2255991) were converted into incremental values 0, 1, and 2 respectively. These values corresponded to the number of chromosomes possessing a minor allele of the SNP. Correlation was examined among 384 subjects at first, and then analyzed among younger and older groups separately after dividing the 384 subjects into those >50 years ($n$ = 309) and ≤50 years ($n$ = 75). Significant association was defined when the given $p$ value of the ANOVA $F$-test was <5% ($p < 0.05$). $\chi^2$ tests were used to ascertain Hardy-Weinberg equilibrium among genotypes ($p > 0.05$). Multiple regression analysis was applied for defining the most significant combination(s) of SNPs that correlate with the adj-aBMD, using Instat 3 software.

## RESULTS

We first clarified the allelic frequencies and heterozygosities of the 13 SNPs in QPCT locus by genotyping 384 subjects (Table 3). The maximal likelihood haplotype frequencies estimated by the expectation-maximization algorithm indicated that two major haplotypes covered 66% of the chromosomes in our test population, suggesting strong LD within the locus. Strong LD was verified over the entire gene locus by evaluating the indices of $D'$ and $r^2$ (Fig. 1).

Analysis on the possible correlations between each SNP and the adj-aBMD revealed that many of the 13 SNPs significantly correlated with adjusted values of forearm aBMD (summarized in Table 3). For example, for SNP −1844C>T, located 1844 bp upstream from the initiation codon ATG (referenced contig NT_005367.1 from GenBank), the minor $T$ allele showed a possible co-dominant effect on lowering adj-aBMD levels ($r$ = 0.17, $p$ = 0.0006; $n$ = 384), because homozygous carriers of the $T$ allele had the lowest adj-aBMD (0.372 ± 0.059 g/cm$^2$, $n$ = 47), heterozygous individuals had intermediate (0.400 ± 0.055 g/cm$^2$; $n$ = 177) adj-aBMD, and homozygous $C$ allele carriers had the highest adj-aBMD (0.406 ± 0.050 g/cm$^2$; $n$ = 160; Fig. 2A). When a recessive effect of the minor $C$ allele was assumed, the significance was more impressive ($p$ = 0.0002, Student's $t$-test). Similar but more prominent results were obtained for R54W (+160C>T; $r$ = 0.18, $p$ = 0.0003; $n$ = 384) as well as for the other two SNPs (+126C>T and IVS2−42A>G). Homozygous carriers (R/R) of the major $C$ allele (corresponding to the first nucleotide in an arginine codon, $C$gg) had the highest adj-aBMD levels (0.407 ± 0.051 g/cm$^2$; $n$ = 159), heterozygous individuals (R/W) had intermediate (0.400 ± 0.056 g/cm$^2$; $n$ = 177) levels, and homozygous $G$ allele carriers (W/W) had the lowest adj-aBMD (0.373 ± 0.058 g/cm$^2$;

TABLE 3. SUMMARY OF CORRELATION ANALYSIS

| *No.* | *Name* | *nt.* | *Allele frequency (heterozygosity)* | n* | *Correlation coefficient (r†)* | p *Value‡* |
|---|---|---|---|---|---|---|
| 1 | −2300C>T | C/T | 0.65:0.35 (46.2%) | 383 | 0.17 | 0.0007 |
| 2 | −1844C>T | C/T | 0.65:0.35 (46.1%) | 384 | 0.17 | 0.0006 |
| 3 | −1095T>C | T/C | 0.65:0.35 (46.2%) | 384 | 0.17 | 0.0007 |
| 4 | IVS1+3583C>G | C/G | 0.83:0.17 (27.9%) | 384 | 0.08 | NS |
| 5 | IVS1−3796A>G | A/G | 0.84:0.16 (26.3%) | 369 | 0.01 | NS |
| 6 | IVS1−1629G>C | G/C | 0.95:0.05 (10.0%) | 381 | 0.02 | NS |
| 7 | +126C>T (Y42Y) | C/T | 0.64:0.36 (45.9%) | 381 | 0.19 | 0.0003 |
| 8 | +160C>T (R54W) | C/T | 0.64:0.36 (45.9%) | 384 | 0.18 | 0.0003 |
| 9 | IVS2−42A>G | A/G | 0.61:0.39 (43.2%) | 370 | 0.19 | 0.0003 |
| 10 | IVS4+974G>A | G/A | 0.58:0.42 (49.5%) | 382 | 0.15 | 0.003 |
| 11 | IVS4+1053T>C | T/C | 0.53:0.47 (50.9%) | 383 | 0.12 | 0.02 |
| 12 | IVS4−1132C>A | C/A | 0.95:0.05 (8.7%) | 381 | 0.04 | NS |
| 13 | IVS6+73A>G | A/G | 0.55:0.45 (47.2%) | 381 | 0.04 | NS |

*Number of genotyped subjects.
†Absolute values of correlation coefficient.
‡*p* values are calculated for regression analysis with ANOVA *F*-test.
NS, not significant.

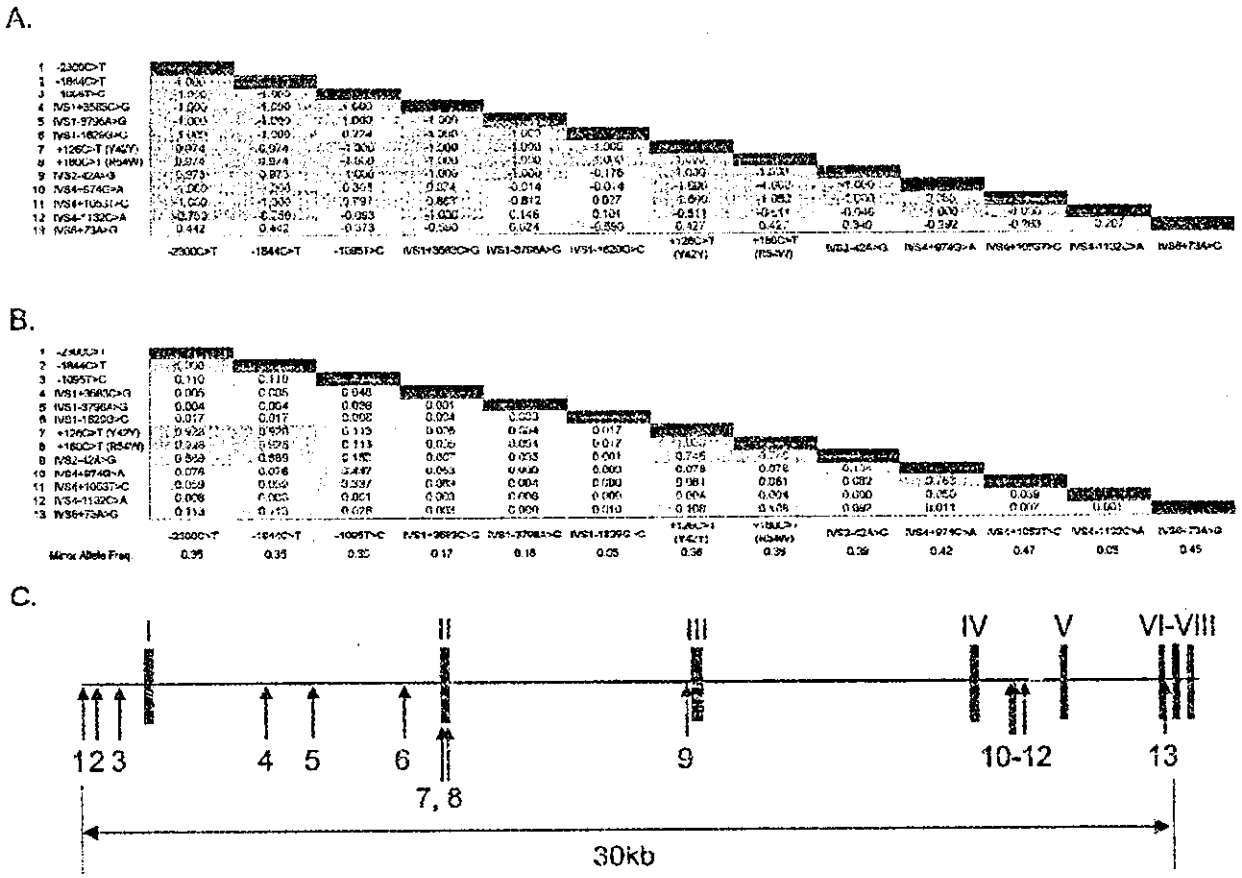


**FIG. 1.** Haplotype and linkage disequilibrium analysis of 13 SNPs localized within the *QPCT* locus. (A) An index of linkage disequilibrium, *D'*, calculated in every possible pair of the 13 SNPs was indicated in each cell. The *D'* values >0.5 are highlighted with gray halftone with gradient. (B) An index of linkage disequilibrium, $r^2$, calculated in every possible pair was indicated. The $r^2$ values >0.1 are highlighted with gray halftone. These indices were calculated on the base of 17 predicted major haplotypes covering 89% of the chromosomes. (C) The schematic diagram of the *QPCT* gene structure indicates locations of the eight exons and the 13 tested SNPs by upward arrows.

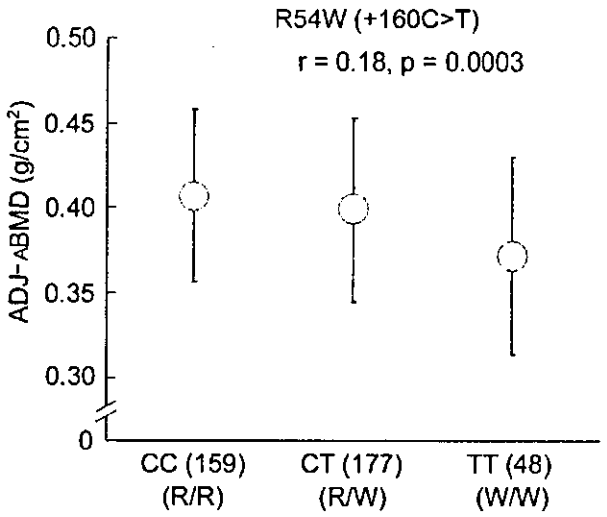


FIG. 2. Association of R54W variation plotted as adj-aBMD of three genotypically classified subgroups among 384 subjects. Circles indicate mean values, and error bars indicate SD. Correlation between numbers of minor alleles and adj-aBMD (g/cm$^2$) was tested by linear regression analysis (R54W, $r = 0.17$, $p = 0.0003$).

$n = 48$; Fig. 2B). As a whole, four SNPs (−2300C>T, −1844C>T, −1095T>C, and R54W) were likely to have functional significance because of their location and the alteration in the coded amino acids (Table 2).

The implication that combined effects of these SNPs could determine BMD was tested by multiple regression analysis. Although calculations using data from all 13 SNPs estimated a fitting equation that explained ~4.7% of adj-aBMD variances ($r^2 = 0.047$), the statistical level for fitness of the equation was not significant ($p = 0.17$). Thus, an interactive effect among several SNPs was indicated. This assumption was supported by analysis of the data for two selected SNPs (R54W and −1844C>T), which yielded a better-fitting equation with statistical significance ($r^2 = 0.033$, $p = 0.0015$), or for three selected SNPs (R54W, −1844C>T, and IVS4−1132C>A; $r^2 = 0.038$, $p = 0.0023$). Although the significance levels for these combined analyses were no better than the results obtained for these SNPs singly, we suppose that combined effects of at least two SNPs at the *QPCT* locus might be influencing the radial aBMD in our cohort.

We next tried to define the period when the SNP genotypes might contribute most to lowering adj-aBMD by testing the correlation among younger and older subject groups separately. Significant and consistent correlation was observed for all the SNPs among the older women ($n = 309$), with consistent or better significance levels (−1844C>T: $r = 0.23$, $p = 0.00007$; −1095T>C: $r = 0.22$, $p = 0.0001$; R54W: $r = 0.21$, $p = 0.0003$), whereas in the younger group of subjects ($n = 75$), we found no significant correlation between any of the SNPs and adj-aBMD. These results may indicate that contribution of these SNPs to acquisition of peak bone mass during the growth period was absent or weak.

## DISCUSSION

The work reported here allows us to propose a possible contribution to BMD of polymorphisms in *QPCT*, a novel candidate for osteoporosis susceptibility. Multiple SNPs in this gene revealed significant association with forearm aBMD among adult women from the general population in Japan. Most of these variations were potentially functional, specifically a nonsynonymous coding SNP, R54W (rs2255991), and several SNPs that seemed to be in promoter sequences. QPCT may be an important regulator of estrogen levels. Our data implied involvement of these SNPs in determining radial BMD for women >50 years of age.

The *QPCT* gene is a rationally selected candidate, based on its protective function for pituitary peptide hormones[8−10] and its chromosomal location suggested by QTL analysis in an Asian population.[13] In addition to the apparent candidacy, our results were intriguing because significant correlation was observed mainly in the polymorphisms whose functions are easily assumed. Among 13 SNPs examined, 3 promoter SNPs and 1 missense SNP, R54W, correlated with adj-aBMD. Although the underlying causative variant cannot be elucidated by the genetics alone because of the high LD in the region of analysis, the informatic motif analysis of the promoter sequence using the MatInspector program[24] revealed that the promoter SNP −1844C>T lies within a consensus binding site for estrogen receptors [potential ERE; T*GGGACA*actt*TGA(C/T)CG*tc].[25,26] Theoretically, estrogen should regulate expression of multiple target genes involved in the HPG axis[4,5] through transcriptional activation or repression through estrogen receptors. The *QPCT* gene might be one of those targets. Altered function of the *QPCT* promoter could account for different bone volumes among individuals.

Estrogen is essential for skeletal maturation as well as for maintenance of bone mass in adulthood, especially during the perimenopausal period.[3,16,17] Therefore, factors involved in estrogen homeostasis may affect bone status through both of the mechanisms generally proposed, that is, low acquisition of peak bone mass before skeletal maturation and unbalanced bone turnover.[1] From our study it is not possible to identify a predominantly contributing mechanism by which the *QPCT* variants may have exerted low BMD in our subjects. However, postmenopausal contribution of these common polymorphisms was implied by the results when subjects were divided into groups above or below age 50, because the association was strikingly significant among the older subjects but absent among the younger women. Further investigations in large cohorts with longitudinal studies will be required.

The mechanism by which certain variants contribute to reduced bone mass is not clear. Despite the LD analysis, where a strong correlation between the missense SNP R54W and the promoter SNP −1844C>T was detected, multiple regression analyses still implied a possibility for the combined effect of regulatory SNPs and a coding SNP in *QPCT* exon 2. Functional analyses should be undertaken to include promoter assays and examination of the enzymatic activities of QPCT variants in converting active forms of TRH or GnRH peptides to the protected forms of these

hormones. Reproducible associations among independent cohort(s) should be documented. Nevertheless, our data are the first to indicate a possible contribution of the *QPCT* gene in determining BMD in a general population, and they imply the contribution of multiple polymorphisms within a single gene.

In summary, the results reported here suggest that common polymorphisms in a novel osteoporosis-susceptibility gene, *QPCT*, affect BMD among postmenopausal women in the Japanese population. Because osteoporosis is a multifactorial disease, other genes, especially those involved in regulating levels of sex hormones, should be investigated in this context as well. Such candidates might include cytochrome P450 enzymes, aromatase, steroid hormone hydroxylases, nuclear receptors of steroid hormones, and their target genes or binding factors. The contributions of those factors should clarify the complex mechanism determining BMD in vivo and should help to explain, at least in part, the pathogenesis of postmenopausal osteoporosis. A novel point of view for establishing suitable treatment designs and plans for prevention of the disease could be obtained through such analyses.

## ACKNOWLEDGMENTS

We thank Mina Kodaira, Miho Kawagoe, and Mayumi Tanaka for technical assistance and Naoko Tsuruta for editorial assistance. This work was supported in part by a special grant for Strategic Advanced Research on "Cancer" and "Genome Science" from the Ministry of Education, Science, Sports and Culture of Japan; by a Research Grant for Research from the Ministry of Health and Welfare of Japan; and by a Research for the Future Program Grant of The Japan Society for the Promotion of Science.

## REFERENCES

1. Giguere Y, Rousseau F 2000 The genetics of osteoporosis: "complexities and difficulties." Clin Genet **57**:161–169.
2. Stewart TL, Ralston SH 2000 Role of genetic factors in the pathogenesis of osteoporosis. J Endocrinol **166**:235–245.
3. Armamento-Villareal R, Villareal DT, Avioli LV, Civitelli R 1992 Estrogen status and heredity are major determinants of premenopausal bone mass. J Clin Invest **90**:2464–2471.
4. Herbison AE, Pape JR 2001 New evidence for estrogen receptors in gonadotropin-releasing hormone neurons. Front Neuroendocrinol **22**:292–308.
5. Kang SK, Choi KC, Tai CJ, Auersperg N, Leung PC 2001 Estradiol regulates gonadotropin-releasing hormone (GnRH) and its receptor gene expression and antagonizes the growth inhibitory effects of GnRH in human ovarian surface epithelial and ovarian cancer cells. Endocrinology **142**:580–588.
6. Burns KH, Matzuk M 2002 Genetic models for the study of gonadotropin actions. Endocrinology **143**:2823–2835.
7. Iwasaki H, Emi M, Ezura Y, Ishida R, Kajita M, Kodaira M, Yoshida H, Suzuki T, Hosoi T, Inoue S, Shiraki M, Swensen J, Orimo H 2003 Association of a Trp16Ser variation in the gonadotropin releasing hormone (GnRH) signal peptide with bone mineral density, revealed by SNP-dependent PCR (Sd-PCR) typing. Bone **32**:85–190.
8. Busby WH, Quackenbush GE, Humm J, Youngblood WW, Kizer JS 1987 An enzyme(s) that converts glutaminyl-peptides into pyroglutamyl-peptides—presence in pituitary, brain, adrenal medulla, and lymphocytes. J Biol Chem **262**:8532–8536.
9. Fisher WH, Spiess J 1987 Identification of a mammalian glutaminyl cyclase converting glutaminyl into pyroglutamyl peptides. Proc Natl Acad USA **84**:3628–3632.
10. Schilling S, Hoffmann T, Rosche F, Manhart S, Wasternack C, Demuth HU 2002 Heterologous expression and characterization of human glutaminyl cyclase: Evidence for a disulfide bond with importance for catalytic activity. Biochemistry **41**:10849–10857.
11. Cummins PM, O'Connor B 1998 Pyroglutamyl peptidase: An overview of the three known enzymatic forms. Biochim Biophys Acta **1429**:1–17.
12. Niu T, Chen C, Cordell H, Yang J, Wang B, Wang Z, Fang Z, Schork NJ, Rosen CJ, Xu X 1999 A genome-wide scan for loci linked to forearm bone mineral density. Hum Genet **104**:226–233.
13. Devoto M, Shimoya K, Caminis J, Ott J, Tenenhouse A, Whyte MP, Sereda L, Hall S, Considine E, Williams JC, Tromp G, Kuivaniemi H, Ala-Kokko L, Prockop DJ, Spotila LD 1998 First-stage autosomal genome screen in extended pedigrees suggests genes predisposing to low bone mineral density on chromosomes 1p, 2p and 4q. Eur J Hum Genet **6**:151–157.
14. Kleinbaum DG, Kupper LL, Muller KE 1988 Applied Regression Analysis and Other Multivariate Methods, 2nd ed. PWS-KENT Publishing, Boston, MA, USA, pp. 299–301.
15. Orimo H, Hayashi Y, Fukunaga M, Sone T, Fujiwara M, Shiraki M, Kushida K, Miyamoto S, Soen S, Nishimura J, Oh-hashi Y, Hosoi T, Gorai I, Tanaka H, Igai T, Kishimoto H 2001 Diagnostic criteria for primary osteoporosis: Year 2000 revision. J Bone Miner Metab **19**:331–337.
16. Riggs BL, Khosla S, Melton LJ III 2002 Sex steroids and the construction and conservation of the adult skeleton. Endocr Rev **23**:279–302.
17. Riggs BL, Melton LJ III 1986 Involutional osteoporosis. N Engl J Med **314**:1676–1686.
18. Makridakis NM, Reichardt JK 2001 Multiplex automated primer extension analysis: Simultaneous genotyping of several polymorphisms. Biotechniques **31**:1374–1380.
19. Iwasaki H, Ezura Y, Ishida R, Kajita M, Kodaira M, Knight J, Daniel S, Shi M, Emi M 2002 Accuracy of genotyping for single nucleotide polymorphisms by a microarray-based single nucleotide polymorphism typing method involving hybridization of short allele-specific oligonucleotides. DNA Res **9**:59–62.
20. Mein CA, Barratt BJ, Dunn MG, Siegmund T, Smith AN, Esposito L, Nutland S, Stevens HE, Wilson AJ, Philips MS, Jarvis N, Law S, de Arruda M, Todd JA 2000 Evaluation of single nucleotide polymorphism typing with invader on PCR amplicons and its automation. Genome Res **10**:330–343.
21. Lyamichev V, Mast AL, Hall JG, Prudent JR, Kaiser MW, Takova T, Kwiatkowski RW, Sander TJ, de Arruda M, Arco DA, Neri BP, Brow MA 1999 Polymorphism identification and quantitative detection of genomic DNA by invasive cleavage of oligonucleotide. Nat Biotechnol **17**:292–296.
22. Miller PT, Sardina IB, Saccone NL, Putzel J, Laitinen T, Cao A, Kere J, Pilia G, Rice JP, Kwok PY 2000 Juxtaposed regions of extensive minimal linkage disequilibrium in human Xq25 and Xq28. Nat Genet **25**:324–328.
23. Thompson EA, Deeb S, Walker D, Motulsky AG 1988 The detection of linkage disequilibrium between closely linked markers: RFLPs at the AI-CIII apolipoprotein genes. Am J Hum Genet **42**:113–24.
24. Quandt K, Frech K, Karas H, Wingender E, Werner T 1995 MatInd and MatInspector: New fast and versatile tools for detection of consensus matches in nucleotide sequence data. Nucleic Acids Res **23**:4878–4884.
25. Klinge CM 2001 Estrogen receptor interaction with estrogen response elements. Nucleic Acids Res **29**:2905–2919.
26. Driscoll MD, Sathya G, Muyan M, Klinge CM, Hilf R, Bambara RA 1998 Sequence requirements for estrogen receptor binding to estrogen response elements. J Biol Chem **273**:29321–29330.

Address reprint requests to:
*Mitsuru Emi, MD, PhD*
*Department of Molecular Biology*
*Institute of Gerontology*
*Nippon Medical School*
*1-396, Kosugi-cho, Nakahara-ku*
*Kawasaki 211-8533, Japan*
*E-mail: memi@nms.ac.jp*

Received in original form October 27, 2003; in revised form February 27, 2004; accepted March 29, 2004.

*Geriatrics and Gerontology International 2004; 4: 245–249*

ORIGINAL ARTICLE

# Association of a single-nucleotide polymorphism in the promoter region of leukemia inhibitory factor receptor gene with low bone mineral density in adult women

Yoshihiro Sudo,[1,5] Yoichi Ezura,[1] Ryota Ishida,[1,5] Mitsuko Kajita,[1] Hideyo Yoshida,[2] Takao Suzuki,[2] Takayuki Hosoi,[2] Satoshi Inoue,[3] Masataka Shiraki,[4] Hajime Orimo,[2] Hiromoto Ito[5] and Mitsuru Emi[1]

[1]*Department of Molecular Biology, Institute of Gerontology, Nippon Medical School, Kawasaki,* [2]*Tokyo Metropolitan Institute of Gerontology and Geriatric Hospital,* [3]*Department of Geriatric Medicine, Faculty of Medicine, University of Tokyo, and* [5]*Department of Orthopaedics, Nippon Medical School, Tokyo and* [4]*Research Institute and Practice for Involutional Diseases, Nagano, Japan*

**Background:** Osteoporosis is believed to result from the interaction among multiple environmental and genetic determinants that regulate bone-mineral density (BMD).

**Methods:** To investigate a potentially predisposing genetic factor in the onset of osteoporosis, we looked for a possible association between BMD in adult Japanese women and known polymorphisms in the leukemia inhibitory factor receptor gene (LIFR).

**Results:** An association analysis of chromosomes from 384 volunteer subjects revealed significant correlation between the −603T > C variant of LIFR and radial BMD ($r = 0.11$, $P = 0.032$) in this test population. Comparisons of mean values of adjusted radial BMD among separate genotypic groups implied an allelic dosage effect, because homozygous carriers of T alleles of that SNP had the highest adjusted BMDs ($0.403 \pm 0.054$ g/cm$^2$); women homozygous for the C-allele had the lowest ($0.373 \pm 0.042$ g/cm$^2$), and heterozygous individuals had intermediate scores ($0.394 \pm 0.056$ g/cm$^2$).

**Conclusion:** This polymorphism in *LIFR* may be an important determinant of predisposition to postmenopausal osteoporosis.

**Keywords:** bone mineral density, leukemia inhibitory factor receptor (LIFR), osteoporosis, regression analysis, single-nucleotide polymorphism.

## Introduction

Osteoporosis is characterized by low bone-mineral density (BMD) and by deterioration of the microarchitecture of bone tissue, with a consequent increase in fragility and susceptibility to fracture. BMD, an important predictor of fracture, is probably determined by genetic as well as environmental factors.[1,2] Any genes that might affect BMD are candidates for involvement in susceptibility to osteoporosis.

Several genes have already been investigated as potential risk factors for osteoporosis.[3,4] For example, cytokine pathways that include interleukin-1 (IL1), interleukin-6 (IL6) and tumor-necrosis factor alpha (TNFα) are considered to be among the most potent of all bone-resorbing mechanisms.[5–8] However, an extended panel of genes must be examined in detail, in view of the polygenic nature of BMD distribution and the multiplicity of endocrine and local factors that are

Accepted for publication 27 May 2004.

Correspondence: Dr Mitsuru Emi MD, PhD, Department of Molecular Biology, Institute of Gerontology, Nippon Medical School, 1-396, Kosugi-cho, Nakahara-ku, Kawasaki 211-8533 Japan. Email: memi@nms.ac.jp

known to influence bone mass and regulate bone turnover.

The leukemia inhibitory factor (LIF) is one such multifunctional cytokine belonging to the IL-6 family.[9,10] It affects the differentiation, survival and proliferation of a wide range of cells, including those in bone tissue. For example, adult mice respond to an excess of circulating LIF with increased numbers of osteoblasts, resulting in overgrowth of mineralized bone.[11] Therefore, we previously searched for common variations in this gene locus (*LIF*) as a candidate gene for osteoporosis susceptibility.[10] However, since only four variations were detected in the 3'-untranslated region of the third exon in our test samples, we excluded *LIF* from the most likely candidates to be examined for association.

Considerable evidence now indicates that LIF activity in bone exerts significant effects through a high-affinity receptor complex composed of a low-affinity LIF-binding subunit (LIFR) and a converter subunit, gp130.[9] Targeted disruption of the LIFR gene in mice causes loss of bone density and increasing numbers of osteoclasts.[1] A linkage study on the rare human diseases Stüve–Wiedemann Syndrome (SWS) and Schwartz–Jampel type 2 syndrome (SJS2) representing long bone bowing and cortical thickening with flared metaphyses identified its mutations in the LIFR gene.[12] Given these observations, we hypothesized that LIFR might be one of the most important elements for determining BMD levels in humans.

To investigate a possible association between genetic variations in LIFR and BMD, we examined five single-nucleotide polymorphisms (SNPs) in the promoter region of this gene, and one missense coding SNP, for association with radial BMD levels among adult women in Japan.

## Materials and methods

### *Subjects*

DNA samples were obtained from the peripheral blood of 384 Japanese women. All participants were non-related volunteers and gave informed consent prior to the study. None had medical complications or were undergoing treatment for conditions known to affect bone metabolism, such as pituitary diseases, hyperthyroidism, primary hyperparathyroidism, renal failure or adrenal or rheumatic diseases, and none was receiving estrogen-replacement therapy. Mean ages and body-mass indices (BMI) with standard deviations (SD) were, respectively, $58.4 \pm 8.6$ years (range, 32–69) and $23.7 \pm 3.61$ kg/cm$^2$ (range, 14.7–38.5).

The BMD (expressed in g/cm$^2$) of each participant was measured in the distal radius by dual-energy X-ray absorptiometry (DEXA) using a DTX-200 osteometer (Meditech Inc., Hawthorne, CA), according to the Guidelines for Osteoporosis Screening in a health check-up program in Japan. To calculate adjusted BMD, measured BMD values were normalized for differences in age and body-mass index (BMI) by multiple regression analysis using the Instat3 software package (GraphPad Software, San Diego, CA).[13,14] The adjustment equation for the study samples was as follows: (adjusted BMD in g/cm$^2$) = (measured BMD in g/cm$^2$) $- 0.006375 \times (58.39 -$ [age in years]) $+ 0.008961 \times (23.65 -$ [BMI in kg/cm$^2$]).

### *Genotyping for molecular variants in the LIFR gene*

We examined six SNPs (−1226T > C, −631C > T, −603T > C, −264C > T, −210G > C, and +1899 A > G (Ile633Met), all archived in the NCBI database (http://www.ncbi.nlm.nih.gov/SNP). All were confirmed to be polymorphic in our test population (Table 1). A contiguous-sequence, NT_023195.12 from RefSeq, was referenced for denoting positions of these SNPs.

Genotypes were determined using the Sd-PCR method, a refined allele-specific PCR, to discriminate polymorphic sequences.[12] In brief, two allele-specific (AS) forward primers and one reverse primer were prepared for each SNP, to transform nucleotide sequences (G, A, T or C) between two alleles at a single site into size-differences. Two different nucleotide mismatches were incorporated at the 3' end of the polymorphic (forward) primers, according to the concept we described elsewhere.[13] AS primers (long and short) have a

**Table 1** Summary of examined polymorphism in the LIFR locus

| No | SNP name† | JSNP-ID‡ | dbSNP§ | Allele frequency | Percent heterozygosity |
|---|---|---|---|---|---|
| 1 | −1226T > C | IMS-JST006591 | rs2071233 | 0.82 : 0.18 | 30 |
| 2 | −631C > T | IMS-JST006592 | rs2071234 | 0.81 : 0.19 | 31 |
| 3 | −603T > C | IMS-JST006593 | rs2071235 | 0.82 : 0.18 | 30 |
| 4 | −264C > T | IMS-JST006594 | rs2071236 | 0.64 : 0.36 | 41 |
| 5 | −210G > C | IMS-JST006595 | rs2071237 | 0.67 : 0.33 | 43 |
| 6 | Ile633Met | IMS-JST060529 | rs2770361 | 0.96 : 0.04 | 7 |

†Location of the SNP was defined by NT_023195.12 from RefSeq; ‡ID number for JSNP database; §ID number for dbSNP (NCBI).

five-base difference between them, and each has a polymorphic nucleotide of the SNP sequence at its 3′ end as well as having an additional artificial mismatch introduced near the 3′ end. The following primer sets allowed distinct discrimination of alleles:

For SNP −210G > C, long AS-primer; 5′-TTTTTG GTAAAAAGCTTTTGCCTCCCGGC-3′, short AS-primer; 5′-CCTAAAAAGCTTTTGCCTCCCGGC-3′, reverse primer; 5′-GTTTGCTGCTAAGATTACCTAT TGTGG-3′. For SNP − 264C > T, Long AS-primer; 5′-TTTTTGGAGCAGTGTGTTTCAGATGGCAG-3′, short AS-primer; 5′-CCAGCAGTGTGTTTCAGATG TTAA-3′, reverse primer; 5′- GTTTGCTGCTAAGATT ACCTATTGTGG − 3′. For SNP −603T > C, Long AS-primer; 5′-TTTTTGGATCCACCTGCCTCGGCCTC GCAA-3′, short AS-primer; 5′-CCATCCACCTGCCTC GGCCTCCGAG-3′, reverse primer; 5′-GTTTGCT GCTAAGATTACCTATTGTGG-3′. For SNP −631C > T, long AS-primer; 5′-TTTTTGGGGGATGACAGG CGTGAGCTACC-3′, short AS-primer; 5′-CCGGGAT GACAGGCGTGAGCCGCT-3′, reverse primer; 5′-CCAGGAAAGTTTGCATTGCTAATA-3′. For SNP − 1226T > C, long AS-primer; 5′-TTTTTGGCAGTG TAAAATCGCCCTTGCCA-3′, short AS-primer; 5′-CCCAGTGTAAAATCGCCCTTATCG-3′, reverse primer; 5′-GTTTGCTGCTAAGATTACCTATTGTGG-3′. For SNP I633M, long AS-primer; 5′-TTTTTGG TCCCATCCCAACAACTTGCTCT-3′, short AS-primer; 5′-CCTCCCATCCCAACAACTTGTCCC-3′, reverse primer; 5′-GCTCTAGGTTTATCTAGTTTGA GCA-3′.

Polymerase chain reactions were performed using 10 ng of each genomic DNA sample and 250 nmol/L of each primer (two polymorphic forward, and a reverse) in a 10-μL reaction mixture containing 10 mmol/L dNTPs, 10 mmol/L Tris-HCl, 1.5 mmol/L $MgCl_2$, 50 mmol/L KCl, 1 U Taq DNA polymerase and 0.5 mmol/L fluorescently labeled dCTP (ROX-dCTP; Perkin-Elmer, Norwalk, CT). The reactions and discrimination of alleles on the ABI Prism 377 DNA system (Applied Biosystems, Foster City, CA) were carried out as described previously.[13]

### *Statistical analysis*

BMD data for each subject were normalized according to age and BMI.[13] Quantitative associations between genotypes and adjusted BMD values (gm/cm$^2$) were evaluated by one-way ANOVA, with regression analysis as a post-hoc test. Three genotypic categories of each SNP were converted into incremental values (0, 1 and 2) corresponding to the number of chromosomes possessing a minor allele. Statistical significance was determined by ANOVA *F*-tests. We used $\chi^2$ tests to ascertain Hardy–Weinberg equilibrium among genotypes. Haplotypes and indices of linkage disequilibrium (LD) were calculated using Arlequine software (Genetics and Biometry Laboratory, Geneva, Switzerland).

## Results

We examined the LIFR gene for possible association with BMD because it was one of the most likely candidates for involvement in susceptibility to osteoporosis. We first confirmed the polymorphic nature of six archived SNPs in that gene among 32 chromosomes from our test population. Since five SNPs in the promoter region (1226T > C, −631C > T −603T > C, −264C > T, −210G > C) and a non-synonymous coding SNP, + 1899 A > G (Ile633Met), were moderately polymorphic, we examined them in our entire panel of 384 subjects and clarified allelic and genotypic frequencies (Table 1). For estimating haplotypes we used only the available genotypic data for the five promoter SNPs in 369 subjects. Results for the missense coding SNP were excluded because its minor allele was so rare (4%). LD within the locus was evaluated by two indices, D′ and $r^2$, calculated for every possible combination of the five SNPs (Fig. 1) LD among these SNPs was evident when D′ > 0.5 and $r^2$ > 0.15.

D′

| | | | | | |
|---|---|---|---|---|---|
| -1226T>C | | | | | |
| -631C>T | 0.991 | | | | |
| -603T>C | -0.918 | -0.972 | | | |
| -264C>T | 0.841 | 0.872 | -0.846 | | |
| -210G>C | -0.939 | -0.884 | 0.936 | 0.749 | |
| | -1226T>C | -631C>T | -603T>C | -264C>T | -210G>C |

$r^2$

| | | | | | |
|---|---|---|---|---|---|
| -1226T>C | | | | | |
| -631C>T | 0.891 | | | | |
| -603T>C | 0.82 | 0.882 | | | |
| -264C>T | 0.088 | 0.104 | 0.091 | | |
| -210G>C | 0.097 | 0.096 | 0.099 | 0.153 | |
| | -1226T>C | -631C>T | -603T>C | -264C>T | -210G>C |

**Figure 1** Linkage disequilibrium (LD) analysis found significant linkage disequilibrium within the LIFR locus: Indices of LD, D′ and $r^2$ based on 17 estimated haplotypes (covering 100% of the chromosomes) constructed with five promoter SNPs were presented in separate tables. D′ greater than 0.4 and $r^2$ values greater than 0.1 are highlighted with gray halftone.

**Table 2** Regression analysis of adjusted bone mass density (BMD) among 384 screening subjects

| SNP Name | $n^{\dagger}$ | Adjusted BMD (g/cm$^2$) Major homozygous (*n*) | Heterozygous (*n*) | Minor homozygous (*n*) | Correlation coefficient (r) | *P*-value$^{\ddagger}$ |
|---|---|---|---|---|---|---|
| −1226T > C | 382 | 0.401 ± 0.054 (256) | 0.394 ± 0.056 (115) | 0.386 ± 0.048 (11) | −0.07 | 0.16 |
| −631C > T | 383 | 0.402 ± 0.054 (250) | 0.395 ± 0.056 (117) | 0.377 ± 0.045 (16) | −0.10 | 0.054 |
| −603T > C | 383 | 0.403 ± 0.054 (255) | 0.394 ± 0.056 (115) | 0.373 ± 0.042 (13) | −0.11 | 0.032 |
| −264C > T | 382 | 0.396 ± 0.055 (167) | 0.399 ± 0.049 (155) | 0.406 ± 0.064 (60) | 0.06 | 0.28 |
| −210G > C | 373 | 0.401 ± 0.055 (169) | 0.398 ± 0.053 (160) | 0.400 ± 0.060 (44) | −0.02 | 0.65 |
| Ile633Met | 383 | 0.400 ± 0.054 (354) | 0.395 ± 0.056 (28) | (–) | 0.02 | 0.63 |

$^{\dagger}$Number of genotyped subjects; $^{\ddagger}$*P*-values are calculated for the regression analysis with ANOVA *F*-test.

**Table 3** Summary of characteristics among 383 subjects subgrouped by −603T > C genotypes

| | T/T | T/C | C/C | Correlation coefficient (r) |
|---|---|---|---|---|
| $n^{\dagger}$ | 255 | 115 | 13 | NA |
| Age (year) | 58.65 ± 8.68 | 57.68 ± 8.44 | 60.23 ± 8.01 | 0.02 |
| Height (cm) | 151.55 ± 6.08 | 151.55 ± 6.09 | 151.55 ± 6.10 | 0.05 |
| Weight (kg) | 54.09 ± 9.15 | 54.57 ± 8.48 | 54.03 ± 7.80 | 0.02 |
| Body mass index (kg/cm$^2$) | 23.54 ± 3.70 | 23.92 ± 3.43 | 23.97 ± 3.34 | 0.05 |

Values are expressed as means ± SDs. Statistical significance for the correlation was tested by ANOVA *F*-test ($P < 0.05$); none of the correlations were statistically significant.
$^{\dagger}$Number of genotyped subjects.

Regression analysis was performed for each SNP by examining correlations between genotypes and adjusted BMDs. Although no significant correlation was evident for five of the six SNPs examined, one promoter SNP (−603T > C) did reveal a significant correlation (r = 0.11, $P = 0.032$) (Table 2). Homozygous carriers of the T allele at this site had the highest adjusted BMDs (0.403 ± 0.054 g/cm$^2$); heterozygous individuals were intermediate (0.394 ± 0.056 g/cm$^2$); homozygous C-allele carriers had the lowest adjusted BMDs (0.373 ± 0.042 g/cm$^2$). The apparent allelic-dosage effect of this variation implied a biological influence on BMD. To examine if −603T > C correlate with the other body status, SNP association was tested for multiple clinical features. As indicated, no significant correlation was detected (age, body weight, height, BMI), indicating a specific effect of this SNP on BMD determination (Table 3).

## Discussion

In the work reported here we found an association of the −603T > C variation of the LIFR gene with radial BMD in adult Japanese women. Adjusted BMD was highest in homozygous T-allele carriers, intermediate among heterozygotes, and lowest among homozygous C-allele carriers. The data implied that variation(s) in the promoter of LIFR might affect bone metabolism, eventually introducing variations in BMD among adult women.

Lowered BMD can result from accelerated bone loss and/or lesser acquisition of bone mass.[1,15] Bone-resorbing effects of cytokine signaling pathways involving IL-1, IL-6, and TNFα have been investigated in vivo and in vitro.[5–8] Since members of the IL-6 family, such as LIF, are known to affect the genesis of osteoclasts, promoter variations in the gene encoding the LIF receptor could influence those activities and bring about changes in BMD. Inadequate transcriptional regulation of LIFR in homozygous carriers of the C allele at the −603 position may have led to increased bone loss for those women. We propose that LIF- and LIFR-signaling cascades should be considered in any studies of osteoclastogenesis. Of course, the effects of these molecules on bone formation will need to be clarified as well, because the present study does not address the question of how this particular SNP functionally affects BMD.

In addition to the correlation between one promoter SNP and adjusted BMD in our test population, we demonstrated LD between all five of the promoter SNPs, most significantly between −1226T > C, −631C > T and −603T > C. Although no significant correlation was evident between genotypes of the first two of those three SNPs and adjusted BMD, it remains possible that they can influence regulation of BMD through a combined effect with the −603 site.

The −603T > C variation is important on theoretical grounds, because a predictive analysis of binding motifs for transcription factors using the MatInspector program v2.2[16] revealed that the sequence surrounding this polymorphic site is sufficiently similar to the consensus binding sequence for a transcription factor, Nkx-2.5 (CAAAGTG, where the underlined A is a variant nucleotide). This putative binding site on the promoter of LIFR was intact on chromosomes carrying the −603T allele, but absent in homozygous carriers of C alleles. Although the functions of human Nkx-2.5 in bone tissues are not yet defined, LIFR might be one of its transcriptional targets.[17] Functional studies on this promoter region are ongoing in our laboratory, however, because physiological roles of single *cis*-element or *trans*-factor could not easily be determined by a simple assay, those studies would be presented in a future independent report. There also exists the possibility that the −603 polymorphism could be in linkage disequilibrium with unknown but functional variants nearby.

In summary, we showed a significant association between the −603T > C variation in the promoter region of the LIFR gene and radial BMD among adult Japanese women. Structural inspection proposed a possible contribution of a transcription factor, Nkx-2.5, that might bind to this SNP site. Functional biological studies as well as longitudinal studies may clarify the true mechanism of the association reported here.

## Acknowledgments

This work was supported in part by a special grant for Strategic Advanced Research on 'Cancer' and 'Genome Science' from the Ministry of Education, Science, Sports and Culture of Japan; by a Research Grant for Research from the Ministry of Health and Welfare of Japan; and by a Research for the Future Program Grant of The Japan Society for the Promotion of Science.

## References

1 Carol BW, Mark CH, Blair RR, Joan SH, Denny L. Targeted disruption of the low-affinity leukemia inhibitory factor receptor gene causes placental, skeletal, neural and metabolic defects and results in perinatal death. *Development* 1995; **121**: 1283–1299.
2 Orimo H, Hayashi Y, Fukunaga M *et al.* Diagnostic criteria for primary osteoporosis: year 2000 revision. *J Bone Miner Metab* 2001; **19**: 331–337.
3 Giguere Y, Rousseau F. The genetics of osteoporosis: 'complexities and difficulties'. *Clin Genet* 2000; **57**: 161–169.
4 Riggs BL, Melton LJ 3rd. Involutional osteoporosis. *N Engl J Med* 1986; **314**: 1676–1686.
5 Boyle WJ, Simonet WS, Lacey DL. Osteoclast differentiation and activation. *Nature* 2003; **423**: 337–342.
6 Jilka RL. Biology of the basic multicellular unit and the pathophysiology of osteoporosis. *Med Pediatr Oncol* 2003; **41**: 182–185.
7 Manolagas SC, Jilka RL. Bone marrow, cytokines, and bone remodeling. Emerging insights into the pathophysiology of osteoporosis. *N Engl J Med* 1995; **332**: 305–311.
8 Pfeilschifter J, Koditz R, Pfohl M, Schatz H. Changes in proinflamatory cytokine activity after menopause. *Endocrine Rev* 2002; **23**: 90–119.
9 Heinrich PC, Behermann I, Haan S, Hermanns HM, Muller NG, Schaper F. Principles of interleukin (IL)-6-type cytokine signalling and its regulation. *Biochem J* 2003; **374**: 1–20.
10 Ishida R, Ezura Y, Iwasaki H *et al.* Linkage disequilibrium and haplotype analysis among four novel single-nucleotide polymorphisms in the human leukemia inhibitory factor (LIF) gene. *J Hum Genet* 2001; **46**: 557–559.
11 Metcalf D, Gearing DP. A myelosclerotic syndrome in mice engrafted with cells producing high levels of leukemia inhibitory factor (LIF). *Leukemia* 1989; **3**: 847–852.
12 Dagoneau N, Scheffer D, Huber C *et al.* Null leukemia inhibitory factor receptor (LIFR) mutations in Stuve-Wiedemann/Schwartz–Jampel type 2 syndrome. *Am J Hum Genet* 2004; **74**: 298–305.
13 Iwasaki H, Emi M, Ezura Y *et al.* Association of a Trp16Ser variation in the gonadotropin releasing hormone signal peptide with bone mineral density, revealed by SNP-dependent PCR typing. *Bone* 2003; **32**: 185–190.
14 Kleinbaum DG, Kupper LL, Muller KE. *Applied Regression Analysis and Other Multivariate Methods*, 2nd edn. Boston: PWS-KENT Publishing, 1988; 299–301.
15 Stewart TL, Ralston SH. Role of genetic factors in the pathogenesis of osteoporosis. *J Endocrinol* 2000; **166**: 235–245.
16 Quandt K, Frech K, Karas H, Wingender E, Werner T. MatInd and MatInspector: new fast and versatile tools for detection of consensus matches in nucleotide sequence data. *Nucl Acids Res* 1995; **23**: 4878–4884.
17 Chen CY, Schwartz RJ. Identification of novel DNA binding targets and regulatory domains of a murine tinman homeodomain factor, nkx-2.5. *J Biol Chem* 1995; **270**: 15628–15633.

ELSEVIER

Molecular and Cellular Endocrinology 218 (2004) 147–153

MCE
Molecular and Cellular Endocrinology

www.elsevier.com/locate/mce

# Systemic distribution of estrogen-responsive finger protein (Efp) in human tissues

Norihiro Shimada[a,b,*], Takashi Suzuki[a], Satoshi Inoue[c], Katsuaki Kato[b], Akira Imatani[b], Hitoshi Sekine[b], Syuichi Ohara[b], Tooru Shimosegawa[b], Hironobu Sasano[a]

[a] *Department of Pathology, Tohoku University School of Medicine, 2-1 Seiryo-machi, Aoba-ku, Sendai 980-8575, Japan*
[b] *Department of Gastroenterology, Tohoku University School of Medicine, Sendai, Japan*
[c] *Division of Gene Regulation and Signal Transduction, Research Center for Genomic Medicine, Saitama Medical School, Saitama, Japan*

Received 30 September 2003; accepted 3 December 2003

**Abstract**

Estrogen-responsive finger protein (Efp), a target gene product of estrogen receptor (ER), is considered essential for estrogen-dependent cell proliferation. The biological significance of Efp remains unclear in human tissues, and therefore, we examined systemic distribution of Efp in human adult and fetal tissues using RT-PCR and immunohistochemistry. Efp mRNA expression was marked in the placenta and uterus, high in the thyroid gland, aorta, and spleen in adult, and relatively low in other human adult and fetal tissues examined in this study. Efp immunoreactivity was detected in epithelium of various adult tissues, and was also detected in cytotrophoblasts of the placenta and splenic macrophages. Efp immunolocalization in human fetus was generally similar as that in adult. These Efp-positive cells were previously reported to be associated with ERα and/or ERβ expression. Therefore, these results indicate that Efp is widely expressed and may play important roles in various human tissues possibly through ERs.


*Keywords:* Distribution; Estrogen-responsive finger protein (Efp); Human tissues; Immunohistochemistry; Reverse transcriptase-polymerase chain reaction (RT-PCR)

## 1. Introduction

It is well known that estrogen plays important roles, not only in female reproductive organs but also in various tissues such as bone, liver, central nervous system (CNS) and cardiovascular system (Dickson and Stancel, 2000; Albertazzi and Purdie, 2001). Biological effects of estrogen are mediated through an interaction with the estrogen receptor (ER). Recently, a second ER, ERβ, has been identified in human (Kuiper et al., 1996; Mosselman et al., 1996), and the previously known human ER has been renamed ERα. ERβ is detected in various human tissues, including in both adult and fetus (Taylor and Al-Azzawi, 2000; Takeyama et al., 2001), while ERα is mainly expressed in female reproductive organs. ERs activate transcription by binding to estrogen-responsive elements (EREs) located in the promoter regions of target genes (Tsai and O'Malley, 1994). A variety of estrogenic functions are characterized by the expression of the estrogen-responsive genes following the binding of receptor protein to EREs (Inoue et al., 1993; Orimo et al., 1999).

Estrogen-responsive finger protein (Efp) belongs to a member of RING- finger B-box Coiled-Coil family (Inoue et al., 1993), which is considered to be involved in the regulation of various cellular functions, including cell-cycle regulation and transcription (Saurin et al., 1996). Efp has been isolated by genomic binding site cloning using a recombinant ER protein, and Efp gene has an ERE at the 3′-untranslated region (Inoue et al., 1993). Efp mRNA was also detected in MCF-7 human breast carcinoma cell line, and was rapidly induced by estrogen treatment within 0.5 h (Ikeda et al., 2000). Efp is mainly expressed in female reproductive organs and brain in mice (Orimo et al., 1995), and the study of Efp knockout mice revealed that Efp is essential for cell growth mediated by estrogen in the uterus (Orimo et al., 1999). In human, Efp expression has been reported

* Corresponding author. Tel.: +81-22-717-8050; fax: +81-22-717-8053.
*E-mail address:* nshimada@int3.med.tohoku.ac.jp (N. Shimada).

0303-7207/$ – see front matter © 2004 Elsevier Ireland Ltd. All rights reserved.
doi:10.1016/j.mce.2003.12.008

in breast tissues (Ikeda et al., 2000; Thomson et al., 2001; Urano et al., 2002), and Efp is postulated to be involved in the mammary gland differentiation (Thomson et al., 2001). However, Efp has not been examined in other human tissues, although estrogenic actions have been demonstrated in various human tissues, and the biological significance of Efp in relation to systemic estrogenic actions remains unclear. Therefore, in this study, we examined systemic distribution of Efp in human adult and fetal tissues using reverse transcription/real-time polymerase chain reaction (RT/real-time PCR) and immunohistochemistry.

## 2. Materials and methods

### 2.1. Tissue collection and preparation

Nonpathological human adult tissues ($n = 6$, respectively) were retrieved from autopsy files at Tohoku University Hospital (Sendai, Japan). Specimens of nonneoplastic area of human uterus ($n = 5$) were obtained from women who underwent hysterectomy for cervical carcinoma at the Department of Obstetrics and Gynecology, Tohoku University Hospital, and informed consent was obtained from these patients before the surgery. Human fetal tissues ($n = 5$, respectively) were obtained from fetuses aged 12–21 weeks gestation after elective termination in normal pregnant women at Nagaike Maternal Clinic (Sendai, Japan), and informed consent was obtained before the elective termination. The specimens were fixed in 10% formalin and embedded in paraffin wax. Histological examinations revealed no significant pathologic abnormalities in these tissues.

RT/real-time PCR analyses were also performed using snap-frozen samples stored at −80 °C. The type of tissues and the number of specimens examined in this study were listed in Table 2.

This study protocol was approved by the ethics committee of Tohoku University School of Medicine (Sendai, Japan).

### 2.2. RT/real-time PCR

Total RNAs were isolated using TRIzol regent (Life Technologies Inc., Grand Island, NY, USA), and used for the first-strand cDNA synthesis with Superscript II reverse transcriptase and oligo $(dT)_{12-18}$ primer (Life Technologies Inc., Gaitherburg, MD, USA). The forward and reverse primers for Efp mRNA were designed in the different exon to avoid the amplification of genomic DNA (Table 1). Oligonucleotide primers for glyceraldehyde-3-phosphate dehydrogenase (GAPDH) (Tokunaga et al., 1987) were also used as internal standard in this study.

The Light Cycler System (Roche Diagnositics GmbH, Mannheim, Germany) with FastStart DNA Master SYBER Green I (Roche Diagnostics GmbH) was used to obtain relative levels of Efp mRNA expression by real-time PCR (Dumoulin et al., 2000). An initial denaturing step of 95 °C for 10 min was followed by 40 cycles, respectively, of 95 °C for 15 s; 10 s annealing at 64 °C (Efp) or 60 °C (GAPDH); and extension for 10 s at 72 °C. The fluorescence intensity of the double-strand specific SYBER Green I, which reflects the amount of formed specific PCR products, was read by the Light Cycler at 86 °C after the end of each extension step. After PCR, these products were resolved on a 2% agarose ethidium bromide gel. PCR products were purified and subjected to direct sequencing (ABI PRISM BigDye Terminator Cycle Sequencing Ready Reaction Kit and ABI PRISM 310 Genetic Analyzer, Perkin-Elmer Corp., PE Applied Biosystems, Foster City, CA, USA) to verify amplification of the correct sequences.

As positive controls, breast cancer cell line MCF-7 was used (Ikeda et al., 2000). Negative control experiments lacked cDNA substrate to check for the possibility of exogenous contaminant DNA, and no amplified products were detected. The mRNA levels of Efp were adjusted to the levels of GAPDH and expressed as the ratio per those in MCF-7 (100%).

### 2.3. Immunohistochemistry

Immunohistochemical analysis was performed by employing the streptavidin–biotin amplification method using a Histofine Kit (Nichirei, Tokyo, Japan). The dilution of human Efp monoclonal antibody (Inoue et al., 1993) was 1/5000 in this study. The antigen-antibody complex was visualized with 3,3′-diaminobenzidine (DAB) solution (1 mM DAB, 50 mM Tris–HCl buffer (pH 7.6), and 0.006% $H_2O_2$), and counterstained with methyl green or hematoxylin. Human breast tissues were used as positive control for Efp immunostaining (Ikeda et al., 2000; Thomson et al., 2001). For negative controls, normal mouse IgG instead of the primary antibody was used, and no specific immunoreactivity was detected in these sections. To identify Efp positive cells in the spleen, we also performed immunohistochemistry for CD68 (DAKO, Carpinteria, CA, USA) using the serial sections.

Table 1
Primer sequences utilized in RT/real-time PCR analysis

| cDNA | | Primer sequences (5′–3′) | cDNA position | Size (bp) |
|---|---|---|---|---|
| Efp (D21205) | Forward | AACATCTCTCAAGGCCAAGGT | 1338–1358 | 287 |
| | Reverse | AGATGCCTACCCCACAGAAGT | 1604–1624 | |
| GAPDH (M33197) | Forward | TGAACGGGAAGCTCACTGG | 731–750 | 307 |
| | Reverse | TCCACCACCCTGTTGCTGTA | 1018–1038 | |

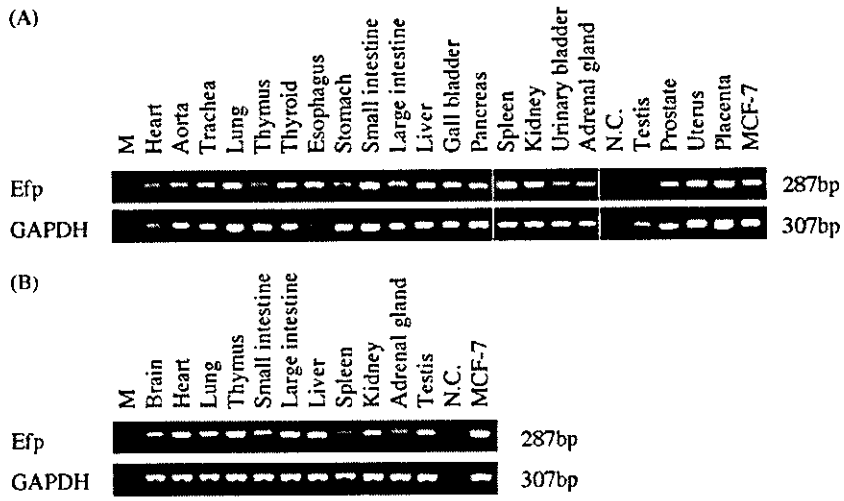


Fig. 1. Reverse transcription/real-time polymerase chain reaction (RT/real-time PCR) analysis for Efp in various human tissues in adult (A) and fetus (B). mRNA expression for Efp was detected as a specific single band (287 bp) in various human tissues both in adult (A) and fetus (B) (upper panels, respectively). Efp mRNA was not detected in adipose tissue in adult. In this study, mRNA expression for glyceraldehyde-3-phosphate dehydrogenase (GAPDH) was also detected as a specific single band (307 bp) in each specimen examined (lower panels, respectively). NC: negative control (no cDNA substrate); MCF-7: positive control. Representative samples were shown in this agarose gel photo.

## 3. Results

### 3.1. RT/real-time PCR

As shown in Fig. 1A and B, mRNA expression for Efp and GAPDH was detected as a specific single band (287 bp for EFP and 307 bp for GAPDH) by RT/real-time PCR analysis. Results of Efp mRNA expression levels in various human tissues were summarized in Table 2. Efp mRNA expression was abundantly detected in the placenta (159.2%) and uterus (95.7%). Efp mRNA expression was also high in the thyroid gland, aorta, and spleen in adult (12.5–12.8%). Efp mRNA expression was relatively low in other human adult and fetal tissues examined ($\leq$10.5%).

### 3.2. Immunohistochemistry

Results of immunohistochemistry for Efp were summarized in Table 3. In adult, Efp immunoreactivity was detected in the cytoplasm of epithelium in various tissues (Fig. 2A–F). In some glandular epithelia, Efp immunoreactivity was tended to be marked at the luminal side (Fig. 2F). In addition, Efp immunoreactivity was detected in the cytotrophoblasts, but not syncytiotrophoblasts (Fig. 2G) of the placenta and vascular endothelium. Efp immunoreactivity was also positive in CD68-positive splenic macrophages in the spleen (Fig. 2H and I).

Patterns of Efp immunolocalization in fetus were generally similar as these in adult (Fig. 2J–L), however, no significant immunoreactivity was detected in the fetal lung, and spleen in this study. Efp immunoreactivity was detected in chondrocytes of cartilage in fetus, whereas it was not significant in adult cartilage.

Table 2
Efp mRNA expression in human tissues

| Tissues | Adult | | Fetus | |
|---|---|---|---|---|
| | *n* | mRNA level (%) | *n* | mRNA level (%) |
| Placenta | 4 | 159.2 ± 98.6 | NA | |
| Uterus | 5 | 95.7 ± 34.4 | NA | |
| Testis | 1 | 7.9 | 1 | 2.0 |
| Prostate | 3 | 4.9 ± 3.6 | NA | |
| Thyroid gland | 6 | 12.5 ± 7.5 | NA | |
| Adrenal gland | 5 | 3.5 ± 2.0 | 1 | 0.2 |
| Brain | NA | | 1 | 1.4 |
| Heart | 4 | 7.1 ± 3.0 | 2 | 3.7 ± 0.9 |
| Aorta | 2 | 12.8 ± 7.9 | NA | |
| Trachea | 3 | 8.4 ± 4.2 | NA | |
| Lung | 5 | 5.3 ± 3.4 | 2 | 8.2 ± 3.8 |
| Thymus | 1 | 3.6 | 2 | 8.2 ± 3.1 |
| Esophagus | 3 | 1.1 ± 1.1 | NA | |
| Stomach | 4 | 0.5 ± 0.4 | NA | |
| Small intestine | 5 | 1.3 ± 0.8 | 1 | 0.8 |
| Large intestine | 5 | 3.1 ± 1.8 | 1 | 9.5 |
| Liver | 5 | 4.6 ± 3.1 | 3 | 5.9 ± 2.3 |
| Gall bladder | 3 | 2.0 ± 1.6 | NA | |
| Pancreas | 3 | 6.1 ± 3.4 | NA | |
| Spleen | 6 | 12.8 ± 7.6 | 1 | 0.1 |
| Kidney | 6 | 10.5 ± 5.9 | 2 | 1.2 ± 0.7 |
| Urinary bladder | 1 | 0.6 | NA | |

The mRNA level of Efp was summarized as a ratio of GAPDH and evaluated as a ratio (%) compared with that of positive control (MCF-7 cells = 100%). Data represent mean ± S.E.M. (more than two samples) or mean ± percent difference (two samples). NA: samples were not available.

## 4. Discussion

In this study, Efp mRNA was abundantly detected in the placenta (cytotrophoblasts) and uterus (endometrial glandular or epithelial cells). In the placenta, estrogen is gen-

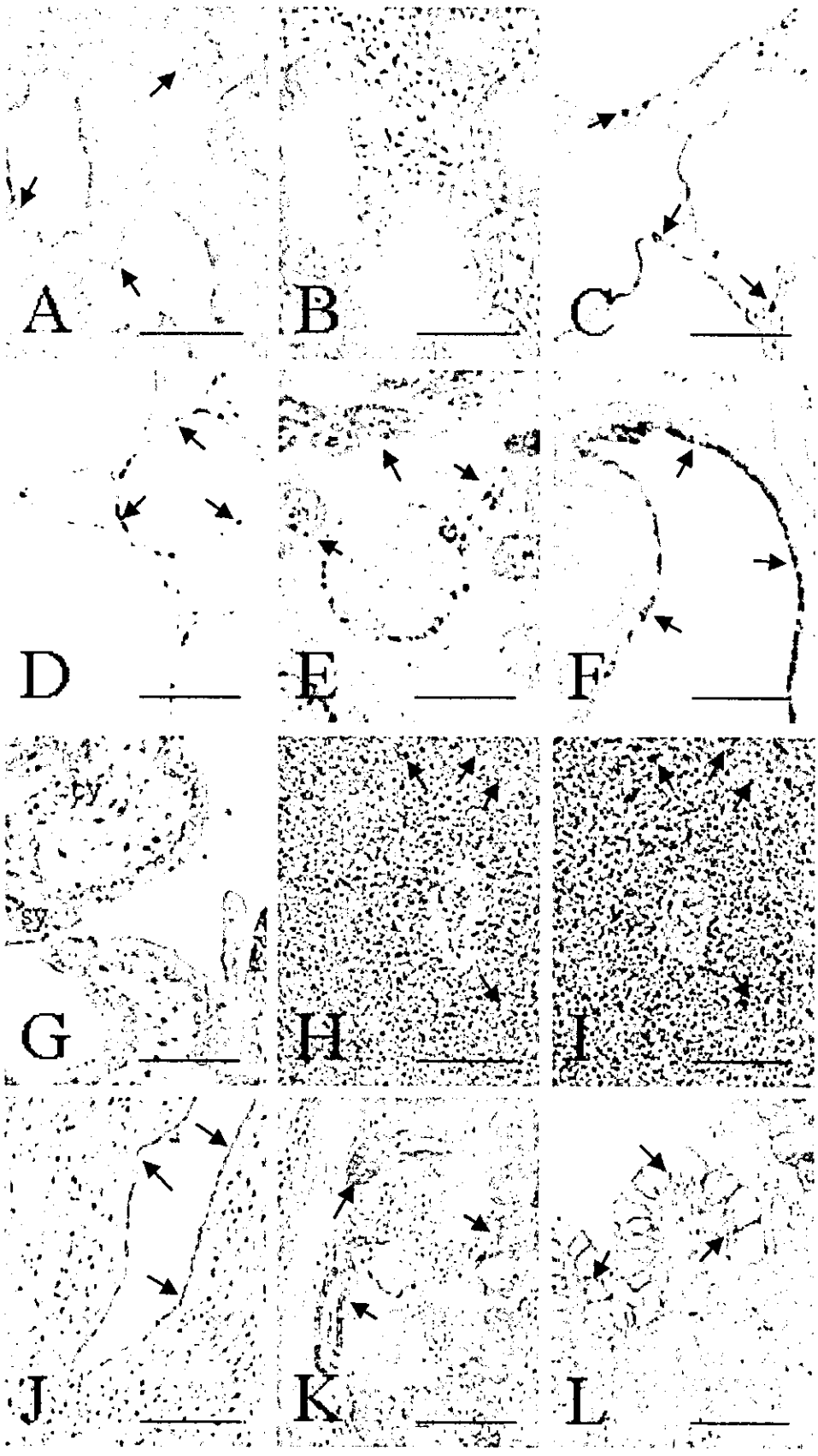
A
B
C
D
E
F
cy
sy
G
H
I
J
K
L